CHAPTER 1

AN EVALUATION OF THE THEORIES OF DIRECT ELECTRON PAIR PRODUCTION (DPP) BY MUONS

1.1 Introduction

Direct production of electron pairs by high energy charged particles in collision with other charged particles (atomic nucleus or electrons) continues to be a subject of interest and importance in high energy physics. Monoenergetic accelerator muons and very high energy cosmic ray muons from greatly inclined directions or at great depths underground are the suitable particles for the investigation of the direct pair production (DPP) process at high energy transfer.

The early theoretical treatments of the process as given by Fury and Carlson, Landau and Lifschitz(1934), Heitler and Nordheim(1934), Nordheim(1935), Bhabha(1935), Nishina et al(1935) and Racah(1937) do not show close agreement at least among a few of these. Bhabha's treatment is the most familiar one and the theoretical results for the case of muon-nucleus collision have been presented in Rossi's High Energy Particles(1952). Murota, Ueda and Tanaka(MUT) (1956) were the first to give a quantum electrodynamic(QED) treatment of the DPP process using the Feynman-Dyson (FD) method. Subsequent work in the FD method of Tarnovskii(1960), Zapolsky(1962), Kel'ner(1967), Kel'ner and Kotov(1968) and Kokoulin Petrukhin (KP) (1970) is believed to give an exact description of the process at both small and large energy

transfer. Probably, there is a need for a critical analysis of the more familiar treatment of Bhabha and the recent refined calculations in order to place in the proper context the state of the theory of the process of direct production of electron pairs.

1.2 Theory of DPP process

An electron pair creation in the coulomb field of a nucleus can be caused by the impact of a high energy charged particle or through absorption of a gamma-ray photon with the threshold value of energy equal to rest mass energy of two electrons. The threshold value for producing a pair in the field of a free electron is equal to four times the electron rest mass energy. According to Dirac's theory, the process is interpreted as a transition of an ordinary electron from a state of negative energy to a state of positive energy under the perturbing influence of two colliding particles. The differential cross section for the creation of a pair by the collision of fast charged particles was derived in the classical and QED calculations. Among the classical treatment the calculation of Bhabha went farther than other calculations in considering the effect of screening and in including certain other aspects. We will discuss and present the theoretical results of Bhabha's calculation and each of QED calculations.

The notation and units used in the various treatments are not the same. For convenience of reference, we used same notations and units. The case considered here is the DPP interaction between an incident muon (m_μ,e) and an atomic nucleus (M,Ze). The relativistic energy, momentum and velocity of the incident muon before and after the collision are denoted by E, p, v and E', p', v' respectively. The energy and momentum of the created electron and positron are denoted by ϵ_-, p_-, and ϵ_+, p_+ respectively. The total energy of the pair is $\epsilon = \epsilon_+ + \epsilon_-$. The rest mass of the electron is m. The velocity is expressed, in unit of velocity c of light, as $\beta = \frac{v}{c}$. The relativistic energy in unit of rest mass energy is expressed by $\gamma = (1-\beta^2)^{-1/2}$. Other physical constants that recur are fine structure constant $\alpha' = 1/137$ and classical radius of the electron r_0 ($=2.82 \times 10^{-13}$cm). Two additional symbols used are

$$u = \frac{\epsilon_+ + \epsilon_-}{E} = \frac{\epsilon}{E}, \quad v = \frac{\epsilon_- - \epsilon_+}{\epsilon_- + \epsilon_+}$$

The relativistic conditions used in all the derivations are

$$E, E' \gg m_\mu c^2, \quad \epsilon_-, \epsilon_+ \gg mc^2$$

These conditions require the ranges of v and u given by $|v| \ll 1 - \frac{nmc^2}{Eu}$ and $\frac{2nmc^2}{E} \leqslant u \leqslant 1 - m_\mu c^2/E$ with $n > 1$.

1.3 The calculation of Bhabha

The procedure adopted by Bhabha consists in calculating the probability of transition of an electron from initial state of negative energy to a final state of positive

energy by impact of the incident particle passing through the coulomb field of the nucleus at rest at a definite impact parameter. The calculation was done under Born approximation. Two processes, known as the first order process and second order process are considered for the transition from initial to final state. In the first order process, the electron in the negative energy state may either interact with one of the colliding particles and jump at once to its final state, the colliding particle going over to an intermediate state. This colliding particle then interacts with the other colliding particle and both jump to their final state. This process involves only one matrix element of interaction of the electron of the produced pair of the colliding particles.

In the second order process the electron in the negative energy state may interact with one of the colliding particle and jump to an intermediate state, after which its interaction with the other colliding particle causes it to its final state. Bhabha treated the two colliding particles classically and neglected the first order process at high energy of the incident particle. Using Born approximation method, he calculated the differential DPP cross section under the relativistic conditions stated above. He derived cross sections for three regions of energy transfer as specified below

Region I-A Very low energy pair of kinetic energy given by

$$p_-,\ p_+ \ll mc$$

The kinetic energy of the pair $\epsilon_k = \frac{1}{2m}(p_-^2 + p_+^2)$.

Region I-B Intermediate energy pair with energy transfer given by $mc^2 << \epsilon_-, \epsilon_+ << \gamma mc^2$

Total energy of the pair $\epsilon = \epsilon_+ + \epsilon_-$

In the calculation, the terms of the order of

$$\left(\frac{\epsilon_+}{\gamma}\right)^2, \left(\frac{\epsilon_-}{\gamma}\right)^2, \left(\frac{m^2c^4}{\epsilon_+}\right)^2, \left(\frac{m^2c^4}{\epsilon_-}\right)^2$$

were neglected.

Region II High energy pair with electron energies in the range given by

$$\gamma m << \epsilon_+, \epsilon_- << E$$

In the calculation, the terms of the order of mc^2 were neglected compared to ϵ_+/γ and ϵ_-/γ

and in each case the effect of screening of the coulomb field of the nuclear charge by the atomic electron has been calculated on the basis of Thomas-Fermi model of the atom. This screening effect was taken into account by introducing in the differential cross section a factor $[1-F(q^2)]$ where the atomic form factor is defined by

$$F(q^2) = \frac{1}{Z}\int \rho(x)\, e^{-z(\epsilon, x)/\hbar}\, dx \qquad (1.1)$$

where $\rho(x)$ is the density of electrons in the atom of nuclear charge Ze and x is measured in unit of distance.

$$r_a = \frac{1}{\alpha'^2}\cdot r_e Z^{-1/3}$$

$$= \frac{1}{\alpha'}\left(\frac{\hbar}{mc}\right) Z^{-1/3}$$

where r_a is the effective radius of the atom according to Thomas-Fermi(TF) model. The form factor $F(q^2)$ is determined from the TF model ($\rho(r)$). It therefore follows from equation (1.1) that the screening effect of the electrons is appreciable when $F(q^2)$ is non-zero in the region determined by $q \leqslant \frac{\hbar}{r_a}$. In Bhabha's paper, the lowest value δ of q for each of three energy transfer region IA, IB, II was derived. When $\delta r_a \gg \hbar$ the form factor $F \ll 1$ and screening effect of the electrons is negligible. On the other hand their effect becomes appreciable if $\delta r_a \leqslant \hbar$. In the very low pair energy region (p_-, $p_+ \ll m$), $\delta \approx 2mc$ is greater than $\hbar/r_a$ and so the screening has no effect. For other two regions the conditions for screening are summarised below for convenience of reference.

Pair energy range	δ	No Screening (NS)
$mc^2 < \epsilon_+, \epsilon_- < \gamma mc^2$	$= m^2/2 \cdot \frac{\epsilon_+ + \epsilon_-}{\epsilon_+ \epsilon_-} \cdot c^3$	$= \epsilon < \frac{2}{\alpha} \cdot Z^{-1/3} mc$
$\gamma mc^2 < \epsilon_+, \epsilon_- < E$	$= \frac{\epsilon}{2} \cdot \frac{1}{\gamma^2}$	$= u > 2\alpha' Z^{1/3} mc\gamma^2$

In the following we present the differential cross section expressions for the second order process for the cases considered above.

(a) creation of slow pairs

The kinetic energy ϵ_K of the created pair is small compared with the electron rest mass energy $\epsilon_K \ll mc^2$. The differential cross section for the creation of such

a pair with kinetic energy between ϵ_k and $\epsilon_k + d\epsilon_k$ is given by

$$d\sigma = \frac{1}{32}(z\alpha' r_0)^2 \left\{ \ln\left(\frac{E}{m_\mu}\right)^2 - \frac{161}{60} + \mathbf{c} \right\} \frac{\epsilon_k^3 \, d\epsilon_k}{m^4 c^8} \quad \ldots (1.2)$$

where

$$\mathbf{c} = \frac{4\gamma^2}{1-\gamma^2} \ln \frac{1}{\gamma^2} - \frac{4}{3}\gamma^2 + \frac{1}{6}\gamma^4$$

This is the equation (30) in Bhabha's paper after neglect of two small factors at high incident energy ($\gamma \geqslant 10, E \geqslant 1\text{GeV}$). The positron and the electron emerge at angles independent of one another and the probability is greatest for their being emitted perpendicular to the path of the incident particle. ~~(b) Creation~~

(b) Creation of intermediate energy pairs $(mc^2 \ll \epsilon_+, \epsilon_- \ll \gamma mc^2)$

The differential cross section as derived by Bhabha equation (32) in his paper is

$$d\sigma = \frac{8}{\pi}(z\alpha' r_0)^2 \frac{\epsilon_+^2 + \epsilon_-^2 + \frac{2}{3}\epsilon_+\epsilon_-}{(\epsilon_+ + \epsilon_-)^4} \ln \frac{K\epsilon_+\epsilon_-}{(\epsilon_+ + \epsilon_-)mc^2} \ln \frac{K' mc^2}{\gamma(\epsilon_+ + \epsilon_-)} d\epsilon_+ d\epsilon_- \quad \ldots\ldots (1.3)$$

where k, k'_ are two numbers of the order of unity arising from some out off introduced in the calculations. In terms of variables u,v this expression becomes

$$d\sigma(u,v) = \frac{4}{3\pi}(z\alpha' r_0)^2 \frac{du\,dv}{u}\left(1 + \frac{v^2}{2}\right) \ln\left(\frac{K'}{u}\frac{m}{m_\mu}\right) \ln\left\{\frac{KuE(1-v^2)}{4mc^2}\right\} \quad \ldots\ldots\ldots (1.4)$$

$$\left(u < \frac{2}{\alpha'} \cdot Z^{-1/3} \cdot \frac{mc^2}{E}\right) \quad \ldots \text{NS}$$

the variable v takes into account the assymetry in the distribution of energy transfer ϵ between the two paired electrons. There is a tendency for one particle to get more energy than the other and this increases with the increasing energy transfer ϵ . At low energy transfer $\epsilon\ (<2mc^2)$, v is negligible. Bhabha, under this assumption, integrated the equation (1.3) over all ϵ_+ for the same ϵ and obtained the following cross section equation (34) in his paper.

$$d\sigma = \frac{56}{9\pi}\left(Z\alpha' r_0\right)^2 \ln\frac{K\epsilon}{mc^2}\ln\frac{K'E}{\left(\frac{m_\mu}{m}\right)\epsilon}\frac{d\epsilon}{\epsilon} \qquad (1.5)$$

$$\left(\epsilon < \frac{2}{\alpha'}\cdot Z^{-1/3}\cdot mc^2\right) \ldots\ldots (NS)$$

It is necessary, however, to integrate the equation(1.4) numerically over its appropriate limits $|v| \leq 1 - \frac{nmc^2}{u\epsilon}$, n=4. The cross section formula thus derived for the screened nuclear coulomb field for energy limited by the condition

$$\epsilon < 2/\alpha' \cdot Z^{-1/3}\cdot mc^2$$

is

$$d\sigma = \frac{1}{3\pi}\left(Z\alpha' r_0\right)^2 \frac{du\,dv}{u}\ln\left(\frac{K'm}{u\,m_\mu}\right)\left(1+\frac{v^2}{2}\right)\ln\left(\frac{K}{\alpha'}\cdot Z^{-1/3}\right) \qquad (1.6)$$

$$\left(u > \frac{2}{\alpha'}\cdot Z^{-1/3}\cdot\frac{mc^2}{E}\right) \ldots\ldots \text{Screening (S)}$$

(c) Creation of high energy pairs $(\gamma mc^2 \ll \epsilon_-, \epsilon_+ \ll \gamma m_\mu c^2)$

The condition of no screening in the case of high energy pair is

$$u > 2\alpha' Z^{1/3}\frac{m}{m_\mu}\cdot\gamma$$

and the differential cross section valid under this condition is

$$d\sigma = \frac{4}{\pi}\left(Z\alpha' r_0\right)^2 \frac{du\,dv}{E^2u^3}\left(\frac{m}{m_\mu}\right)\ln\left(\frac{2KE}{m_\mu}\right) \qquad (1.7a)$$

For the case of effective screening the cross section is

$$d\sigma = \frac{4}{\pi}\left(Z\alpha' r_0\right)^2 \frac{du\,dv}{E^2 u^3}\left(\frac{m}{m_\mu}\right) \ln\left(k\frac{Z^{-1/3}}{\alpha'}\cdot u\,\frac{m_\mu}{m}\right) \qquad (1.7b)$$

The screening effect replaces only the expression under the logarithm in equation (1.7). For larger energy transfer the difference between the two expressions is very small.

The relativistic energy ranges of validity for each of the cross section formulae do not allow us to integrate the differential cross sections over v in the limits -1 to +1 as was done by Davisson (1952) (High Energy Particles by Rossi). The limits of v have been fixed in the present work by assigning a minimum value of 4 mc^2 for ϵ_+ or ϵ_- in accordance with the relativistic requirements of the calculations as specified by Bhabha. As already mentioned Bhabha's calculations are based on Born approximation. The conditions of applicibility of Born approximation are

$$\frac{Ze^2}{\hbar v_-}, \frac{Ze^2}{\hbar v_+} \ll 1$$

$$\text{or, } \frac{\alpha' Z}{\beta_-}, \frac{\alpha' Z}{\beta_+} \ll 1$$

in the relativistic energy regions $\beta_- \approx \beta_+ \approx 1$.
So the condition for the validity becomes $\alpha' Z \ll 1$
This conditions is satisfied if Z is small. For lead(Z=82), , $\alpha' Z$ =0.6 and for aluminium (Z=13), $\alpha' Z$ = 0.09. The cross section formulae are also applicable when the primary

particle is an electron. In this case the energy range under the case (c) does not exist. The effect of the exchange of the primary electron on the electron of the created pair was neglected in the procedure adopted by Bhabha. Its effect, however, is small for small apir energy and large initial energy of the electron.

Bhabha's formula(32) equation (1.3) has an extra logarithemic term than that in the first BPF cross section formula given by Fury and Carlson. It, however, agrees with the formula obtained by Landau(1934).

1.4 The treatment of Kurota, Ueda and Tanaka (KUT)

The authors calculated DPP cross sections by using the FD method. In this method incident charged particle is treated quantum electrodynamically, but a target particle is regarded as a fixed coulomb field.

The FD interaction diagrams for the DPP process are shown in Fig.1.1. The calculations were done under the usual relativistic condition and the approximation of small angles between the incident and target particles. They determined separately the contributions from (i) the case when spin of the incident particle does not flip and polarization of virtual photons is transverse (ii) the spin flips and polarization of virtual photons is transverse and (iii) the spin does not flip and polarization of virtual photons is longitudional. The spin flips and the longitudional pola-

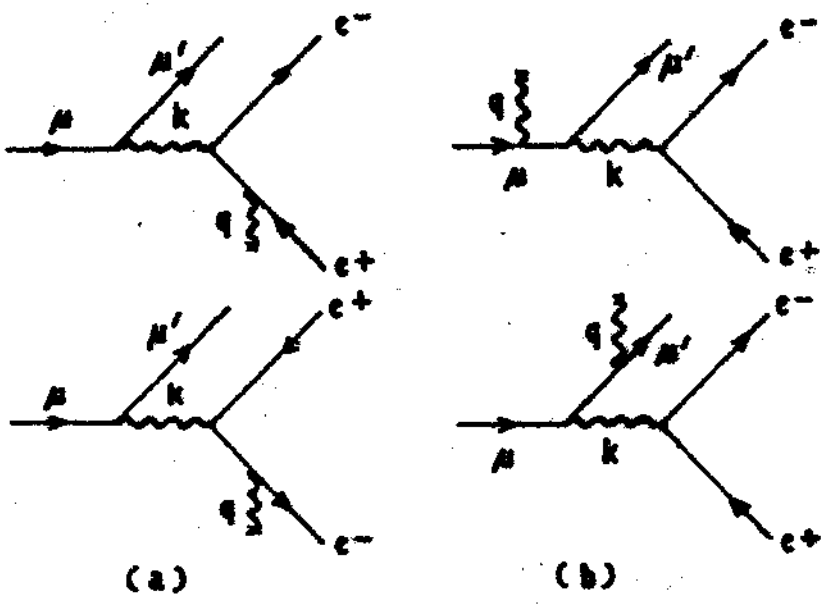

Figure I'1. The Feynman-Dyson diagrams for pair production. (a) Second order process. (b) First order process.

risation case was neglected in their calculations. In order to calculate the differential cross section irrespective of angles at which the created electrons appears the usual angular integration was done under the small angle approximation mentioned above. In this process an arbitrary number α of the order of unity was introduced as a cut off parameter for angular integration.

As in Bhabha's treatment the screening effect was taken into account by introducing the factor $[1-F(q^2)]$ in the differential cross section and by making the similar consideration about the relation between momentum transfer q and the effective TF radius of the atom r_a . The minimum value of q in their treatment is given by

$$q_{min} = \frac{2}{u(1-v^2)} \cdot (mc^2)^2/E \cdot (1+x)$$

where

$$x = \left(\frac{m_\mu}{2m}\right)^2 \frac{u^2(1-v^2)}{1-u}$$

The differential cross section for the second order process (diagram a) in variables u and v in the NS case as obtained from equation (23) of MUT is given by

$$d\sigma(u,v) = \frac{2}{3\pi}\left(Z\alpha' r_0\right)^2 \frac{du\,dv}{u}\Big[\Big\{\Big((2+v^2)+x(3+v^2)\Big)\ln\frac{1+x}{x} - (3+v^2)\Big\}\frac{1+(1-u)^2}{2} + \frac{1-u}{1+x}(1-v^2) + \frac{u^2}{2}\Big\{\frac{x}{1+x} + (2+v^2) - x(3+v^2)\ln\Big(\frac{1+x}{x}\Big)\Big\}\Big] L_1 \qquad (1.8)$$

where

$$L_1 = \ln\left[\frac{\alpha E u(1-v)}{2mc^2 e(1+x)^{1/2}}\right] - 1 \qquad \text{for } q_{min} \gg \alpha' Z^{1/3} mc \text{ (NS)}$$

$$= \ln\left[\frac{\alpha}{\alpha'} Z^{-1/3}(1+x)^{-1/2}\right] \qquad \text{for } q_{min} \ll \alpha' Z^{1/3} mc \text{ (S)}$$

with $e = 2.718$.

For the first order process (diagram b) the differential cross section as equation 42 of MUT in terms of u and v is

$$d\sigma(u,v) = \frac{1}{3\pi}(Z\alpha' r_0)^2\left(\frac{m}{m_\mu}\right)^2 \frac{du\,dv}{u} L_2\Big([\{1+(1-u)^2\}\{(\tfrac{3}{2}+\tfrac{2}{x})\ln(1+x)-2\}-(1-u)\{(1+\tfrac{2}{x})\ln(1+x)-2\}](1+v^2)\Big) \qquad (1.10)$$

where

$$L_2 = \ln\left(\frac{2\alpha E(1-v)}{e u m_\mu c^2 (1+\frac{1}{x})^{1/2}}\right) \qquad \text{for } q_{min} \gg \alpha' Z^{1/3} mc \text{ (NS)} \qquad \ldots\ldots(1.11)$$

$$= \ln\left\{\frac{\alpha}{\alpha'} Z^{-1/3}(1+\tfrac{1}{x})^{1/2}\right\} \qquad \text{for } q_{min} \ll \alpha' Z^{1/3} mc \text{ (S)} \qquad \ldots\ldots(1.11)$$

Following an analysis of MUT formulation by Ueda (one of the authors of MUT formulation), Kobayakawa gave a semi-empirical cross section formula in the following form

$$d\sigma(E,\epsilon) = b_p(E)\,\Phi(u) \qquad (1.12)$$

with

$$b_p(E) = \frac{1.9.27}{\pi}\frac{N}{A}\frac{m}{m_\mu}(Z\alpha' r_0)^2 \frac{\ln E/mc^2 - 2.79}{\ln E/mc^2 - 0.489}\ln\left(\frac{183}{Z^{1/3}}+\frac{9}{16}\right)$$

and

$$\Phi(u) = \delta p(1+\delta p)/u(u+\delta p)$$

where $\delta p = 5.1 \times 10^{-3}$ (Bugaev et al,1970). The first term $b_p(E)$ is the energy loss expression for the pair production by muons and the second term gives the variation of cross section with energy transfer. This cross section expression has been used in the recent investigation.

1.5 Treatment of Ternovskii

Ternovskii considered both the diagrams a and b in Fig.1.1 to calculate the differential cross section with an accuracy better than the calculation of MUT. The condition for calculation was same as those in the MUT calculation. The integration over angles of emission of the electron and the positron was done exactly without introducing any approximation. The result for the second order process can be written,using units $\hbar = c = 1$, in terms of variables u and υ as

$$d\sigma(u,\upsilon) = \frac{1}{3\pi}(Z\alpha' r_0)^2 \frac{du\,d\upsilon}{u} L\Big[\Big\{1+(1-u^2)\Big\}\Big\{(2+\upsilon^2)+(3+u^2)x \ln\left(1+\frac{1}{x}\right) + \frac{2(1-\upsilon^2)(1-u)}{1+x} + u^2\Big\{\frac{x}{1+x} - x\ln(1+x)(3+\upsilon^2) + (2+\upsilon^2)\Big\}\Big] \qquad (1.13)$$

As in the other treatment, the form of the expression is

determined by the conditions of screening and no screening

$$L_a = \ln\left(\frac{uE(1-v^2)}{4m(1+x)^{1/2}}\right) \qquad \text{for } q_{min} > \alpha' Z^{1/3} m \ (NS)$$

$$= \ln\left(\frac{Z^{-1/3}}{\alpha'}(1+x)^{1/2}\right) \qquad \text{for } q_{min} < \alpha' Z^{1/3} m \ (S) \qquad \text{.....(1.14)}$$

with

$$q_{min} = \frac{2}{u(1-v^2)} \frac{m^2(1+x)}{E}$$

when $u \ll m/m_\mu$ (low energy transfer), $x \ll 1$

the differential cross section is

$$d\sigma(u,v) = \frac{4}{3\pi}(Z\alpha' r_0)^2 \frac{du\,dv}{u} L_a\left[(1+v^2)\right] \ln\frac{x}{um} \qquad (1.15)$$

For the first order process (diagram b) the cross section is

$$d\sigma_b = \frac{4}{3\pi}(Z\alpha' r_0)^2 \frac{1}{m^2} \frac{d\epsilon_- d\epsilon_+}{\epsilon^2} \frac{E^2+(E-\epsilon)^2}{p^2} \frac{\epsilon_+^2+\epsilon_-^2}{\epsilon^2}$$

$$\ln\frac{m^2\epsilon_+\epsilon_-}{E(E-\epsilon)} \ln\frac{1}{mRy_{min}} \qquad (1.16)$$

where R is the nuclear radius and

$$y_{min} = \frac{\epsilon m}{E(E-\epsilon)} \qquad \text{for } q_{min} > \alpha' Z^{1/3} m$$

$$= \alpha' Z^{1/3}/m \qquad \text{for } q_{min} < \alpha' Z^{1/3} m$$

1.6 Treatments of Kel'ner(1967), Kel'ner Kotov(1968)

A more exact calculation of DPP cross section in the energy transfer range extending over relativistic region

was done by Kel'ner. Under relativistic energy condition for all the participating particles the main cross section results using the units $\hbar = c = m = 1$ for both NS and S regions are written in the following form

$$d\sigma = \frac{4Z^2}{\pi}\alpha^3 \frac{d\epsilon_+ d\epsilon_-}{\epsilon} \frac{E'}{E}\left\{\Phi_a + \frac{1}{m_\mu^2}\Phi_b\right\} \qquad (1.17)$$

where the functions Φ_a and Φ_b are given by

$$\Phi_{a,b} = L_{a,b} B_{a,b} + \tfrac{1}{2}\Delta_{a,b}$$

The functions Φ_a and Φ_b are different to NS and S region. For Φ_a, NS and S region are distinguished by $\eta_{min} = \frac{\epsilon}{\epsilon_+\epsilon_-}(1+x)$. For NS region $\eta_{min} >> \frac{Z^{1/3}}{137}$ and Φ_a^N is given by

$$B_a^N = \left\{a_1 \ln\left(1+\tfrac{1}{x}\right) - b_1 - \frac{c_1}{1+x}\right\}$$

$$\Delta_a^N = -a_1 f\left(\tfrac{1}{1+x}\right) + b_1 x \ln\left(1+\tfrac{1}{x}\right) + \frac{c_1}{1+x}$$

$$L_a^N = \ln \frac{uE(1-v^2)}{2(1+x)^{1/2}} - \frac{1}{2}$$

For S region $\eta_{min} << \frac{Z^{1/3}}{137}$ and Φ_a^S is given by

$$B_a^S = B_a^N$$

$$\Delta_a^S = a_1 f\left(\tfrac{1}{1+x}\right) - d_1 \ln\left(1+\tfrac{1}{x}\right) - \tfrac{2}{3}\frac{c_1}{1+x} + \tfrac{2}{9}\frac{\epsilon_+\epsilon_-}{\epsilon^2}$$

$$L_a^S = \ln\left(183 Z^{-1/3}\sqrt{1+x}\right)$$

In the above expressions a,b,c,d are given by

$$a_1 = \left\{\left(\frac{\epsilon_+}{\epsilon}\right)^2 + \left(\frac{\epsilon_-}{\epsilon}\right)^2 + \frac{2}{3}\frac{\epsilon_+\epsilon_-}{\epsilon^2}\right\}\left(1 + \frac{\epsilon^2}{\epsilon_+\epsilon_-}\right) + \frac{4}{3}x\left(1 - \frac{\epsilon_+\epsilon_-}{\epsilon^2}\right)$$

$$B_1 = \frac{1}{3}x + \frac{1}{3}\left(\frac{\epsilon_+}{\epsilon} - \frac{\epsilon_-}{\epsilon}\right)^2 + \frac{1}{6}\frac{\epsilon^2}{EE'}$$

$$b_1 = \left(\frac{\epsilon_+}{\epsilon}\right)^2 + \left(\frac{\epsilon_-}{\epsilon}\right)^2 + \frac{2}{3}\frac{\epsilon_+\epsilon_-}{\epsilon^2}$$

$$d_1 = b_1 x + \frac{1}{9}\frac{\epsilon_+\epsilon_-}{\epsilon^2}\left(\frac{E}{E'} + \frac{E'}{E}\right) + \frac{1}{9}x\left(1 + 2\frac{\epsilon_+\epsilon_-}{\epsilon^2}\right)$$

$$x = m^2\frac{\epsilon_+\epsilon_-}{EE'}$$

For the first order process (diagram b) Φ_b^N for the no screening condition $\left(1+\frac{1}{x}\right)m^2\frac{\epsilon}{EE'} >> \frac{Z^{1/3}}{137}$ is given by

$$B_b^N = a_2 \ln(1+x) + b_2\frac{\epsilon_+\epsilon_-}{\epsilon^2} + c_2\frac{x}{1+x}$$

$$\Delta_b^N = -a_2 f\left(\frac{x}{1+x}\right) - b_2\frac{\epsilon_+\epsilon_-}{x\epsilon^2}\ln(1+x) - \frac{c_2 x}{1+x}$$

$$L_b^N = \ln\frac{4E.E'\epsilon_+\epsilon_-}{\epsilon^2(1+x)} - 1$$

and for the screening condition

$$\left(1+\frac{1}{x}\right)m^2\frac{\epsilon}{EE'} << \frac{Z^{1/3}}{137}$$

Φ_b^S is given by

$$B_b^S = B_b^N$$

$$\Delta_b^S = a_2 f\left(\frac{1}{1+x}\right) + d_2\ln(1+x) + \frac{2}{3}\frac{c_2 x}{1+x} + \frac{2}{9}\frac{\epsilon_+\epsilon_-}{\epsilon^2}$$

$$L_b^S = \ln\left[m.183\,Z^{-1/3}\left(1+\frac{1}{x}\right)^{1/2}\right]$$

The expressions for a_2, b_2, c_2, d_2 are given by

$$a_2=\left(\frac{E}{E'}+\frac{E'}{E}-\frac{2}{3}\right)\left(\frac{1}{2}\,\frac{\epsilon_+^2+\epsilon_-^2}{\epsilon^2}-\frac{\epsilon_+\epsilon_-}{\epsilon^2 x}\right)-\frac{1}{3m^2}$$

$$b_2=\frac{E}{E'}+\frac{E'}{E}-\frac{2}{3}$$

$$c_2=\frac{4}{3}\,\frac{\epsilon_+\epsilon_-}{\epsilon^2}-\frac{1}{6}\,\frac{\epsilon^2}{EE'}\left(\frac{\epsilon_+^2+\epsilon_-^2}{\epsilon^2}\right)+\frac{1}{3m^2}$$

$$d_2=b_2\,\frac{\epsilon_+\epsilon_-}{\epsilon^2 x}-\frac{2}{9}\left(\frac{\epsilon_+\epsilon_-}{\epsilon^2 x}-\frac{1}{2}\,\frac{\epsilon_+^2+\epsilon_-^2}{\epsilon^2}\right)+\frac{1}{9m^2}$$

In the NS case and in terms of the variables defined above

$$d\sigma(u,v)=\frac{2}{3\pi}\left(Z\alpha' r_0\right)^2\frac{1-v}{u}\left\{\Phi_a^N+\frac{1}{m^2}\,\Phi_b^N\right\} \qquad (1.18)$$

where

$$\Phi_{a,b}^N = L_{a,b}^N B_{a,b}^N + \frac{1}{2}\,\Delta_{a,b}^N$$

$$B_a^N = \left[\left\{(2+v^2)\left(1+\frac{u^2}{2(1-u)}\right)+x(3+v^2)\right\}\ln\left(1+\frac{1}{x}\right) - (3+v^2)+\frac{1-v^2}{1+x}-\frac{v^2}{2(1-u)(1+x)}\right]$$

$$\Delta_a^N = -\left[\left\{(2+v^2)\left(1+\frac{u^2}{2(1-u)}\right)+x(3+v^2)\right\}f\left(\frac{1}{1+x}\right) + (2+v^2)x\ln\left(1+\frac{1}{x}\right)+\left(x+v^2+\frac{u^2}{2(1-u)}\right)\frac{1}{1+x}\right]$$

$$L_a^N=\left[\ln\frac{E\,u\,(1-v^2)}{2\,(1+x)^{3/2}}-\frac{1}{2}\right]$$

$$B_b^N = 3\Big[\Big\{\Big(\frac{1}{1-u}+(1-u)-\frac{2}{3}\Big)\frac{1}{4}\Big\{(1+v^2)-\frac{1-v^2}{x}\Big\}-\frac{1}{3m^2}\Big]$$
$$\ln(1+x)+\Big[\frac{3}{4}(1-v^2)\Big(\frac{1}{1-u}+(1-u)-\frac{2}{3}\Big)\Big]$$
$$+\Big[(1-v^2)-\frac{1}{2}\frac{u^2}{1-u}\frac{1}{2}(1+v^2)+\frac{1}{m^2}\Big]\frac{x}{1+x}$$

$$\Delta_b^N = -3\Big[\Big\{\frac{1}{1-u}+(1-u)-\frac{2}{3}\Big\}\frac{1}{4}\Big\{(1+v^2)-\frac{1-v^2}{x}\Big\}-\frac{1}{3x^2}\Big]$$
$$f\Big(\frac{1}{1+x}\Big)-\frac{3}{4}\Big[\Big\{\frac{1}{1-u}+(1-u)-\frac{2}{3}\Big\}\frac{(1-v^2)}{x}\ln(1+x)\Big]$$
$$-\Big[(1-v^2)-\frac{1}{4}\frac{u^2}{1-u}(1+v^2)+\frac{1}{m^2}\Big]\frac{x}{1+x}$$

$$L_b^N = \Big[\ln\frac{E^2(1-u)(1-v)}{(1+x)}-1\Big]$$

In the S-case the cross section

$$d\sigma(u,v) = \frac{2}{3\pi}\Big(\frac{Zr_e}{137}\Big)^2\frac{1-u}{u}\Big\{\Phi_a^S+\frac{1}{m^2}\Phi_b^S\Big\} \qquad (1.19)$$

$$\Phi_{a,b}^S = L_{a,b}^S\,B_{a,b}^S+\frac{1}{2}\Delta_{a,b}^S$$

$$B_a^S = B_a^N$$

$$\Delta_a^S = \Big[(2+v^2)\Big(1+\frac{u^2}{2(1-u)}\Big)+x(3+v^2)\Big]f\Big(\frac{1}{1+x}\Big)$$
$$-\Big[(2+v^2)x+\frac{1}{12}(1-v^2)\Big(\frac{1}{1-u}+(1-u)\Big)+\frac{1}{3}x\Big(1+\frac{1-v^2}{2}\Big)\Big]$$
$$\ln\Big(1+\frac{1}{x}\Big)-\frac{2}{3}\Big(x+v^2+\frac{u^2}{2(1-u)}\Big)\frac{1}{1+x}+\frac{1}{6}(1-v^2)$$

$$L_a^S = \ln\left(183\, Z^{-1/3}(1+x)^{1/2}\right)$$

$$B_b^S = B_b^N$$

$$\Delta_b^S = 3\Big[\Big\{\frac{1}{1-u}+(1-u)-\frac{2}{3}\Big\}\frac{1}{4}\Big\{(1+v^2)-\frac{(1-v^2)}{x}\Big\}-\frac{1}{3m^2}\Big]$$
$$f\Big(\frac{1}{1+x}\Big)+\Big[\Big(\frac{1}{1-u}+(1-u)-\frac{2}{3}\Big)\cdot\frac{3}{4}\frac{(1-v^2)}{x}$$
$$-\frac{2}{3}\Big(\frac{1-v^2}{4x}-\frac{1+v^2}{4}\Big)+\frac{1}{3m^2}\Big]\ln(1+x)+2\Big[\frac{1-v^2}{3}-\frac{1}{12}\frac{u^2}{1-u}(1+v^2)$$
$$+\frac{1}{3m^2}\Big]\frac{x}{1+x}+\frac{2}{3}\frac{1-v^2}{4}$$

$$L_b^S = \ln\left(m\,183\,Z^{-1/3}\left(1+\tfrac{1}{x}\right)^{1/2}\right)$$

For low energy transfer $u \ll \frac{1}{m}$, we find $x \ll 1$, the differential cross section under this situation is given by (28) and (40a) of Kel' ner for Φ_a and Φ_b

$$\Phi_a = 3(2+v^2)\Big\{\Big(\ln\big(uE(1-v^2)-\tfrac{1}{2}\big)\Big(\ln\frac{4}{m^2u^2(1-v^2)}-\frac{\pi^2}{12}\Big)$$
$$-v^2\Big\{\ln\big(uE(1-v^2)-1\big)\Big\}$$

$$\Phi_b = x\Big[\Big(1+\frac{1-v^2}{4}\Big)\ln\Big\{E^2(1-v^2)\Big\}-2-\frac{1-v^2}{6}\Big]$$

The differential cross section given is only the sum of the cross section for the second order process (diagram a) and the first order process (diagram b). The contribution to the cross section for interference between the two is nothing for muons in cosmic rays.

Kel'ner Kotov(1968) presented the differential cross section equation (1) in his paper in three variables ϵ_+, ϵ_- and $t\,(=|q^2|)$ valid for relativistic condition(2). They introduced the effect of screening by the atomic electrons and made some simplifications which result in an error of about 3%. The final cross section for the second order process (diagram a) is

$$d\sigma_a = \frac{16}{\pi}\left(Z\alpha' r_0\right)^2 \frac{du}{u} F_a(E,u) \qquad (1.20)$$

The expression for F_a (E,u) for low and high range of u is given for both NS and S regions.

Lower energy transfer region $u \ll \frac{1}{m}$

$$F_a(E,u) = \frac{1}{18}\left\{7\ln(2Eu)\ln\frac{1}{mu} + \frac{10}{3}\ln(2Eu) - \frac{109}{6}\ln\frac{1}{mu} - \frac{811}{36} + \frac{21\pi^2}{24}\right\} \quad \ldots (N)$$

$$= \frac{7}{18}\left[\left(\ln\frac{1}{mu} + \frac{10}{21}\right)\ln 189 Z^{-\frac{1}{3}} + \frac{\pi^2}{24} - \frac{1}{28}\right] \quad \ldots (S)$$

For higher energy transfer range $\left(u \gg \frac{1}{m}\right)$, the expression for F_a (E,u) is given for two limiting cases (a) $t_{min} \ll 1$ (b) $t_{min} \gg 1$ for each of NS and S regions.

For the first order process (diagram b) the cross section is

$$d\sigma_b = \frac{16}{\pi}\left(Z\alpha' r_0\right)^2 \frac{du}{u} F_b(E,u) \qquad 1.21$$

where

$$F_b(E,u) = \frac{1}{12m^2}\left[\left(\frac{4}{3} - \frac{4}{3}u + u^2\right)\left(\ln\frac{m^2u^2}{1-u} - \frac{5}{3}\right) + 1 - \frac{1}{3}(1+u)^2\right]\ln\left\{\frac{Amz^{-1/3}}{\left(A.\sqrt{e}/2.z^{-1/3}\frac{m^2u^2}{E(1-u)}\right)+1}\right\}$$

$$A = 189, \quad e = 2.7189$$

For $u \gg \frac{1}{m}$

$$d\sigma = \frac{16}{\pi}\left(z\alpha r_0\right)^2 \frac{du}{u}\left[F_b(E,u) + F_a(E,u)\right] \qquad (1.22)$$

This can be calculated from a single expression for each of the first and second order processes.

Following Kobayakawa's semi-empérical form equation(1.12) Wright used Kel' ner Kotov(1968) results to obtain

$$\frac{d\sigma(E,e)}{de} = b\rho(E)\,\Phi(u)$$

$$b\rho(E) = \left(0.37\ln\frac{E}{m_\mu} - 0.95\right)\times 10^{-6}\frac{cm^2}{gm} \qquad E < 100\ GeV$$

$$= 2.75\left(\frac{\ln E/m_\mu - 5.43}{\ln E/m_\mu - 4.34}\right)\times 10^{-6}\frac{cm^2}{gm} \qquad 100 < E \leq 5\times 10^4\ GeV$$

and $\Phi(u)$ same as Kobayakawa.

1.7 Treatment of Kokoulin and Petrukhin (1969)

Kokiulin Petrukin (KP) (1969) have given a combined expression of L which gives a smooth transition from

NS region to S region and also gives Kel'ner's expression L_a^N and L_a^S in their appropriate ranges of validity. A parameter τ was defined as

$$\tau = 189/Z^{1/3}$$

and for NS and S regions we have

$\tau \gg 1$ no screening (NS)

$\tau \ll 1$ complete screening (S)

Using this parameter the combined single expression for is

$$L_a = \ln \frac{189\, Z^{-1/3}(1+x)^{1/2}}{1+\tau e^{1/2}}$$

with $e = 2.718$

Taking the correction term Δ_a into account, this gives

$$L_a = \ln \frac{189\, Z^{-1/3}(1+x)^{1/2}(1+Y_a)^{1/2}}{1+\tau e^{1/2}(1+Y_a)}$$

Similarly for the first order process (diagram b)

$$L_b = \ln \frac{189\, m Z^{-1/3}\left(1+\frac{1}{x}\right)^{1/2}(1+Y_b)}{1+\tau e^{1/2}(1+Y_b)}$$

where

$$Y_a = -\frac{5-v^2+4\beta(1+v^2)}{2(1+3\beta)\ln\left(1+\frac{1}{x}\right)-v^2-2\beta(2-v^2)}$$

$$Y_b = \frac{4+v^2+3\beta(1+e^2)}{(1+v^2)\left(\frac{3}{2}+2\beta\right)\ln(3+x)+1-\frac{3}{2}v^2}$$

with

$$\beta = u^2/2(1-u)$$

The final result is

$$d\sigma(u,v) = \frac{2}{3\pi}(Z\alpha r_0)^2 \frac{1-u}{u}\left\{\Phi_a + \frac{1}{m^2}\Phi_b\right\} du\, dv \qquad (1.24)$$

with

$$\Phi_a = \left\{\left[(2+\vartheta^2)\left(1+\frac{u^2}{2(1-u)}\right)+x(3+\vartheta^2)\right]\ln\left(1+\frac{1}{x}\right) + \frac{1-\vartheta^2}{1+x} - \frac{u^2}{2(1-u)(1+x)} - (3+\vartheta^2)\right\} L_a$$

$$\Phi_b = \left\{\left[(1+\vartheta^2)\left(1+\frac{3}{2}\frac{u^2}{2(1-u)}\right) - \frac{1}{x}\left(1+\frac{1}{2}\frac{u^2}{2(1-u)}\right)(1-\vartheta^2)\right] \ln(1+x) + \frac{x(1-\vartheta^2)}{1+x} - \frac{u^2}{2(1-u)}\frac{x}{1+x} + \left(1+\frac{2u^2}{2(1-u)}\right)(1-\vartheta^2)\right\} L_b$$

These expressions for Φ_a, Φ_b are valid for muon energy greater than about 5 GeV and are positive for $u_{min} = 4/E$ and $u_{max} = (E-m)/E$

1.8 Consideration of some other effects

(a) Effect of DPP process in the coulomb field of atomic electrons.

In considering the passage of a primary muon through an atom one must also take into account the DPP process in the coulomb field of atomic electrons. As in the case of bremsstrahlung, contribution of atomic electrons to the DPP process can be taken into account by replacing Z^2 in the differential cross section formula by $\frac{1}{2}(Z+a)$ where the value of a in the case of bremsstrahlung is taken to be close to 1. In the case of DPP process the values of a as calculated by Kel' ner and Kotov (1968) are the following

a = 1 for No screening

$a = \dfrac{\ln 1440\, Z^{-2/3}}{\ln 189\, Z^{-1/3}}$ for total screening

It is therefore evident that in the case of low Z atoms the effect is not negligible.

Rozental(1968) discussed the corrections arising from the DPP contribution of orbital electrons and from the radiative processes he gave the correction term as 0.95 Z(Z+a).

(b) Effect of multiple scattering in the target medium

The cross section of bremsstrahlung and pair production processes are influenced by multiple scattering in the target medium. Landau and Pomeranchuk(1953), Migdale(1957), Ternovskii(1960) considered the effect on the DPP process and found that as in the case of electron bremsstrahlung and photon induced pair production processes(Dovzhenki and Pomanski,1965) the effect is not negligible for energy transfers small compared to primary muon energy (above 10^5 GeV).

(c) The effect of nuclear form-factor

The size of the nucleus of the atom limits the maximum value of momentum transfer to 1/R where $R=0.56\ A^{1/3}$, the radius of the nucleus (A,Z). The nuclear form factor has appreciable effect only if the actual momentum transfer is $q \geq 1/R$

In the theory, maximum value of q is

$$q^2_{max} = \frac{\epsilon_+ \epsilon_-}{E E'} m^2 = 1 + x \approx x \text{ , where } x \gg 1$$

So, nuclear form factor should be taken into account when

$$\frac{\epsilon_+ \epsilon_-}{E E'} >> 1/(mR)^2$$

The cross section in this case is obtained from

$$\Phi_a = \frac{1}{x}\left[1 + \frac{2\epsilon_+\epsilon_-}{\epsilon^2} + \frac{\varepsilon^2}{E E'}\left(\frac{\epsilon_+^2 + \epsilon_-^2}{\epsilon^2}\right)\right] \ln \frac{2EE'}{\varepsilon m^2 R} \qquad (1.26)$$

1.9 Other DPP theories

The treatments discussed above are useful from the view point of practical use. Other calculations include the work of Bjorken and Drell,(1959), Bjorken and Chen,(1967), Jhoneon Jr.,(1965), Brodsky and Teng,(1967), Henry(1967) and Hamma et al(1971). These calculations are based on eight FD diagrams and give completer expressions for differential cross sections. Most of these are not available in a form for numerical evaluation and use in experiments, although they represent considerable improvement in the theory of DPP process.

1.10 Numerical calculations

In order to bring out the differences, if any, among the various theoritical calculations, we have carried out numerical compulations of the differential cross sections for all the formulae discussed above. A selection of the various computed differential cross sections are shown in figs. 1.2 to 1.15.

In each case,computed cross sections have been corrected for the contribution of the DPP process between the incident muons and the atomic electrons using the formula of Kelner Kotov (1968) equation (1.25).

The physical constants used in this compukations are those recommended by the 1973 committee of the International Council of Scientific Union (I C S U).

In each graph the differential energy transfer spectrum according to KP is displayed along with only one of the remaining theoretical formulation under the present consideration. This procedure has brought out the degree of disagreement among the various theoretical proposals. A set of tables of differential cross section are also included to serve the purpose of numerical comparison.

1.11 Discussion

1.11.1 KP cross section with Bhabha cross section (figs1.2 and 1.3, tables 1.1 - 1.6)

It can be seen that at the lower primary energy 10 GeV, the agreement is excellent over the energy transfer range from 5 MeV to 80 MeV both for Al and Pb. With increasing primary energy, the Bhabha cross section in the medium energy transfer range slowly increases over KP cross section. In the higher energy transfer range and lower energy transfer range below 5 MeV, the Bhabha prediction lies lower than the KP prediction.

~~1.11.2~~

TABLE 1.1

DIFFERENTIAL PROBABILITIES FOR MUON INITIATED DPT PROCESS OF ALUMINIUM AT E=10 GeV MUON ENERGY
(cm^2/gm MeV)

Transfered Energy	KP cross section	MUT cross section $\alpha=2$, n =4	MUT cross section $\alpha=1$, n = 4	Kobayakawa cross section derived from (MUT	Ternovskii cross section	Kel'ner cross section	Kelner Kotov cross section	Wright cross section derived from Kelner Kotov	Bhabl cross se
3.16 MeV	6.75×10^{-6}			5.26×10^{-5}		6.75×10^{-6}	5.75×10^{-6}	6.02×10^{-5}	1.32×10^{-6}
5 MeV	1.01×10^{-5}	1.57×10^{-5}	1.04×10^{-5}	3.08×10^{-5}	1.02×10^{-5}	1.01×10^{-5}	9.4×10^{-6}	3.35×10^{-5}	9.77×10^{-6}
10 MeV	7.94×10^{-6}	1.08×10^{-5}	9.97×10^{-6}	1.33×10^{-5}	8.2×10^{-6}	8.35×10^{-6}	7.86×10^{-6}	1.43×10^{-5}	8.17×10^{-6}
20 MeV	4.32×10^{-6}	4.89×10^{-6}	4.43×10^{-6}	5.26×10^{-6}	4.67×10^{-6}	4.54×10^{-6}	4.23×10^{-6}	5.23×10^{-6}	4.45×10^{-6}
40 MeV	1.62×10^{-6}	2.07×10^{-6}	1.71×10^{-6}	1.74×10^{-6}	1.83×10^{-6}	1.70×10^{-6}	1.60×10^{-6}	1.59×10^{-6}	1.62×10^{-6}
80 MeV	4.89×10^{-7}	6.70×10^{-7}	5.61×10^{-7}	4.86×10^{-7}	5.54×10^{-7}	5.13×10^{-7}	4.85×10^{-7}	3.86×10^{-7}	4.58×10^{-7}
100 MeV	3.10×10^{-7}	4.26×10^{-7}	3.92×10^{-7}	2.08×10^{-7}	3.67×10^{-7}	3.18×10^{-7}	3.08×10^{-7}	2.40×10^{-7}	2.43×10^{-7}
200 MeV	5.80×10^{-8}	8.08×10^{-8}	6.96×10^{-8}	5.65×10^{-8}	7.01×10^{-8}	5.85×10^{-8}	6.02×10^{-8}	4.26×10^{-8}	2.70×10^{-8}
400 MeV	9.42×10^{-9}	1.29×10^{-8}	1.12×10^{-8}	9.80×10^{-9}	1.14×10^{-8}	9.15×10^{-9}	9.25×10^{-9}	6.59×10^{-9}	
800 MeV	1.27×10^{-9}	1.69×10^{-9}	1.45×10^{-9}	1.43×10^{-9}	1.51×10^{-9}	1.21×10^{-9}	1.43×10^{-9}	9.28×10^{-10}	
1 GeV	6.35×10^{-10}	8.26×10^{-10}	7.10×10^{-10}	7.84×10^{-10}	7.42×10^{-10}	5.40×10^{-10}	6.10×10^{-10}	4.86×10^{-10}	
2 GeV	6.75×10^{-11}	8.18×10^{-11}	6.75×10^{-11}	1.01×10^{-11}	7.29×10^{-11}	4.45×10^{-11}	6.65×10^{-11}	6.36×10^{-11}	
4 GeV	6.75×10^{-12}	6.89×10^{-12}	5.20×10^{-12}	1.31×10^{-12}	6.02×10^{-12}	5.12×10^{-12}	6.67×10^{-12}	8.17×10^{-12}	

TABLE 1.2

DIFFERENTIAL PROBABILITIES FOR MUON INITIATED DIP PROCESS OF ALUMINIUM AT E = 100 GeV MUON ENERGY

(cm^2/gm MeV)

Transfered Energy		KP cross section	MUT cross section α =2, n =4	MUT cross section α =1, n =4	Kobayakawa cross section derived from MUT	Ternovskii cross section	Kel'ner cross section	'Kel'ner Kotov' cross section	'Wright cross section derived from' 'Kelner Kotov'	Bhabh cross sect
3.16	MeV	1.35×10^{-5}			8.36×10^{-5}		1.35×10^{-5}	1.30×10^{-5}	1.50×10^{-4}	2.43×10^{-6}
5	MeV	1.99×10^{-5}	2.76×10^{-5}	1.88×10^{-5}	5.00×10^{-5}	2.01×10^{-5}	1.99×10^{-5}	1.89×10^{-5}	9.04×10^{-5}	1.97×10^{-5}
10	MeV	1.88×10^{-5}	2.12×10^{-5}	1.57×10^{-5}	2.49×10^{-5}	1.69×10^{-5}	1.89×10^{-5}	1.71×10^{-5}	4.35×10^{-5}	2.02×10^{-5}
20	MeV	1.23×10^{-5}	1.42×10^{-5}	1.01×10^{-5}	1.21×10^{-5}	1.19×10^{-5}	1.29×10^{-5}	1.14×10^{-5}	2.09×10^{-5}	1.37×10^{-5}
40	MeV	6.75×10^{-6}	8.17×10^{-6}	6.65×10^{-6}	5.72×10^{-6}	7.02×10^{-6}	7.35×10^{-6}	6.20×10^{-6}	9.70×10^{-6}	4.92×10^{-6}
80	MeV	3.21×10^{-6}	4.21×10^{-6}	3.48×10^{-6}	2.59×10^{-6}	3.48×10^{-6}	3.73×10^{-6}	2.96×10^{-6}	4.21×10^{-6}	3.59×10^{-6}
100	MeV	2.42×10^{-6}	3.13×10^{-6}	2.57×10^{-6}	1.97×10^{-6}	2.57×10^{-6}	2.72×10^{-6}	2.30×10^{-6}	3.16×10^{-6}	2.75×10^{-6}
200	MeV	9.32×10^{-7}	1.13×10^{-6}	9.50×10^{-7}	7.76×10^{-7}	9.50×10^{-7}	1.05×10^{-6}	9.10×10^{-7}	1.16×10^{-6}	1.10×10^{-6}
400	MeV	3.24×10^{-7}	3.76×10^{-7}	3.10×10^{-7}	2.56×10^{-7}	3.10×10^{-7}	3.68×10^{-7}	3.15×10^{-7}	3.54×10^{-7}	3.62×10^{-7}
800	MeV	8.70×10^{-8}	9.63×10^{-8}	8.08×10^{-8}	7.00×10^{-8}	8.08×10^{-8}	9.40×10^{-8}	8.50×10^{-8}	8.60×10^{-8}	5.10×10^{-8}
1	GeV	5.42×10^{-8}	5.96×10^{-8}	5.02×10^{-8}	4.40×10^{-8}	5.02×10^{-8}	5.80×10^{-8}	5.15×10^{-8}	5.15×10^{-8}	2.50×10^{-8}
2	GeV	1.05×10^{-8}	1.16×10^{-8}	9.80×10^{-9}	8.69×10^{-9}	9.80×10^{-9}	1.13×10^{-8}	1.00×10^{-8}	9.34×10^{-9}	
4	GeV	1.78×10^{-9}	2.02×10^{-9}	1.73×10^{-9}	1.45×10^{-9}	1.73×10^{-9}	1.94×10^{-9}	1.72×10^{-9}	1.45×10^{-9}	
8	GeV	2.43×10^{-10}	2.94×10^{-10}	2.53×10^{-10}	2.12×10^{10}	2.48×10^{-10}	2.74×10^{-10}	2.39×10^{-10}	2.04×10^{-10}	
10	GeV	1.24×10^{-10}	1.56×10^{-10}	1.37×10^{-10}	1.12×10^{-10}	1.31×10^{-10}	1.43×10^{-10}	1.19×10^{-10}	2.34×10^{-10}	
20	GeV	1.32×10^{-11}	1.76×10^{-11}	1.68×10^{-11}	1.40×10^{-11}	1.51×10^{-11}	1.41×10^{-11}	1.39×10^{-11}	1.40×10^{-11}	
40	GeV	1.38×10^{-12}	1.57×10^{-12}	1.42×10^{-12}	1.94×10^{-12}	1.67×10^{-12}	1.98×10^{-12}	1.40×10^{-12}	1.79×10^{-12}	

TABLE 1.3

DIFFERENTIAL PROBABILITIES FOR MUON INITIATED INTERACTION OF ALUMINIUM AT E = 1000 GeV MUON ENERGY
(cm^2/gm MeV)

Transfered Energy	KP cross section	MUT cross section $\alpha = 2$, $n = 4$	MUT cross section $\alpha = 1$, $n = 4$	Kobayakawa cross section derived from MUT	Chernovskii cross section	Kel'ner cross section	Kel'ner Kotov cross section	Wright cross section derived from Kel'ner Kotov	Bhabha cross section
3.16 MeV	2.08×10^{-5}			9.75×10^{-5}		2.08×10^{-5}	2.00×10^{-5}	2.36×10^{-4}	3.54×10^{-6}
5 MeV	3.18×10^{-5}	3.96×10^{-5}	2.69×10^{-5}	6.00×10^{-5}	3.02×10^{-5}	3.18×10^{-5}	2.99×10^{-5}	1.24×10^{-4}	2.97×10^{-5}
10 MeV	3.00×10^{-5}	3.26×10^{-5}	2.34×10^{-5}	2.08×10^{-5}	2.70×10^{-5}	3.08×10^{-5}	2.98×10^{-5}	6.95×10^{-5}	3.24×10^{-5}
20 MeV	2.05×10^{-5}	2.26×10^{-5}	1.72×10^{-5}	1.51×10^{-5}	2.05×10^{-5}	2.24×10^{-5}	2.05×10^{-5}	3.48×10^{-5}	2.25×10^{-5}
40 MeV	1.22×10^{-5}	1.53×10^{-5}	1.17×10^{-5}	7.26×10^{-6}	1.28×10^{-5}	1.36×10^{-5}	1.30×10^{-5}	1.84×10^{-5}	1.34×10^{-5}
80 MeV	6.53×10^{-6}	8.60×10^{-6}	6.94×10^{-6}	3.59×10^{-6}	6.94×10^{-6}	7.64×10^{-6}	6.50×10^{-6}	8.29×10^{-6}	7.30×10^{-6}
100 MeV	5.23×10^{-6}	6.85×10^{-6}	5.61×10^{-6}	2.86×10^{-6}	5.61×10^{-6}	6.13×10^{-6}	5.19×10^{-6}	6.72×10^{-6}	5.97×10^{-6}
200 MeV	2.43×10^{-6}	3.01×10^{-6}	2.48×10^{-6}	1.38×10^{-6}	2.48×10^{-6}	2.71×10^{-6}	2.45×10^{-6}	3.21×10^{-6}	2.91×10^{-6}
400 MeV	1.08×10^{-6}	1.31×10^{-6}	1.05×10^{-6}	6.59×10^{-7}	1.05×10^{-6}	1.18×10^{-6}	1.10×10^{-6}	1.50×10^{-6}	1.34×10^{-6}
800 MeV	4.45×10^{-7}	5.02×10^{-7}	4.31×10^{-7}	2.97×10^{-7}	4.31×10^{-7}	4.64×10^{-7}	4.40×10^{-7}	6.50×10^{-7}	5.48×10^{-7}
1 GeV	3.35×10^{-7}	3.72×10^{-7}	3.08×10^{-7}	2.29×10^{-7}	3.08×10^{-7}	3.48×10^{-7}	3.28×10^{-7}	4.88×10^{-7}	3.98×10^{-7}
2 GeV	1.19×10^{-7}	1.27×10^{-7}	1.06×10^{-7}	8.92×10^{-7}	1.06×10^{-7}	1.19×10^{-7}	1.17×10^{-7}	1.80×10^{-7}	1.19×10^{-7}
4 GeV	3.78×10^{-8}	3.94×10^{-8}	3.29×10^{-8}	2.94×10^{-8}	3.29×10^{-8}	3.76×10^{-8}	3.95×10^{-8}	5.42×10^{-8}	1.95×10^{-8}
8 GeV	1.00×10^{-8}	1.02×10^{-8}	8.59×10^{-9}	8.07×10^{-9}	8.59×10^{-9}	9.70×10^{-9}	1.10×10^{-8}	1.32×10^{-8}	
10 GeV	6.31×10^{-9}	6.36×10^{-9}	5.37×10^{-9}	5.06×10^{-9}	5.37×10^{-9}	6.13×10^{-9}	6.22×10^{-9}	7.96×10^{-9}	
20 GeV	1.22×10^{-9}	1.21×10^{-9}	1.04×10^{-9}	1.00×10^{-9}	1.04×10^{-9}	1.18×10^{-9}	1.26×10^{-9}	1.44×10^{-9}	
40 GeV	2.00×10^{-10}	2.00×10^{-10}	1.74×10^{-10}	1.67×10^{-10}	1.72×10^{-10}	1.94×10^{-10}	2.05×10^{-10}	2.33×10^{-10}	
80 GeV	2.97×10^{-11}	3.02×10^{-11}	2.62×10^{-11}	2.44×10^{-11}	2.72×10^{-11}	2.97×10^{-11}	3.02×10^{-11}	3.13×10^{-11}	
100 GeV	1.59×10^{-11}	1.64×10^{-11}	1.43×10^{-11}	1.29×10^{-11}	1.53×10^{-11}	1.62×10^{-11}	1.65×10^{-11}	1.65×10^{-11}	
200 GeV	1.89×10^{-12}	2.08×10^{-12}	1.78×10^{-12}	1.72×10^{-12}	2.14×10^{-12}	2.08×10^{-12}	2.05×10^{-12}	2.16×10^{-12}	
400 GeV	1.97×10^{-13}	2.64×10^{-13}	9.54×10^{-14}	9.33×10^{-13}	2.74×10^{-13}	2.64×10^{-13}	2.17×10^{-13}	2.75×10^{-13}	

TABLE 1.4

DIFFERENTIAL PROBABILITIES FOR MUON INITIATED DIP PROCESS OF LEAD AT E = 10 GeV MUON ENERGY
(cm^2/gm MeV)

Transfered Energy		PP cross section	MUT cross section $\alpha=2$, n = 4	MUT cross section $\alpha=1$, n = 4	Kobayakawa cross section derived from MUT	Ternovskii cross section	Kelner cross section	Kelner Kotov cross section	Wright cross section derived from Kelner Kotov	Bhabha cross section
3.16	MeV	2.56×10^{-5}			1.86×10^{-4}		2.56×10^{-5}	2.35×10^{-5}	2.19×10^{-4}	4.88×10^{-6}
5	MeV	3.75×10^{-5}	5.81×10^{-5}	3.95×10^{-5}	1.15×10^{-4}	3.80×10^{-5}	3.75×10^{-5}	3.55×10^{-5}	1.12×10^{-4}	3.62×10^{-5}
10	MeV	2.94×10^{-5}	3.95×10^{-5}	2.73×10^{-5}	4.93×10^{-5}	3.03×10^{-5}	3.09×10^{-5}	2.92×10^{-5}	5.28×10^{-5}	3.03×10^{-5}
20	MeV	1.60×10^{-5}	2.01×10^{-5}	1.59×10^{-5}	1.95×10^{-5}	1.73×10^{-5}	1.68×10^{-5}	1.53×10^{-5}	1.95×10^{-5}	1.68×10^{-5}
40	MeV	6.00×10^{-6}	7.68×10^{-6}	6.36×10^{-6}	6.43×10^{-6}	6.78×10^{-6}	6.30×10^{-6}	6.00×10^{-6}	5.93×10^{-6}	6.01×10^{-6}
80	MeV	1.81×10^{-6}	2.84×10^{-6}	2.08×10^{-6}	1.76×10^{-6}	2.05×10^{-6}	1.90×10^{-6}	1.80×10^{-6}	1.43×10^{-6}	1.70×10^{-6}
100	MeV	1.15×10^{-6}	1.58×10^{-6}	1.35×10^{-6}	1.10×10^{-6}	1.36×10^{-6}	1.18×10^{-6}	1.12×10^{-6}	8.73×10^{-7}	9.0×10^{-7}
200	MeV	2.15×10^{-7}	2.99×10^{-7}	2.58×10^{-7}	2.19×10^{-7}	2.60×10^{-7}	2.17×10^{-7}	2.23×10^{-7}	1.58×10^{-7}	9.50×10^{-8}
400	MeV	3.49×10^{-8}	4.78×10^{-8}	4.15×10^{-8}	3.64×10^{-8}	4.22×10^{-8}	3.39×10^{-8}	3.50×10^{-8}	2.45×10^{-8}	
800	MeV	4.70×10^{-9}	6.25×10^{-9}	5.38×10^{-9}	5.30×10^{-9}	5.59×10^{-9}	4.47×10^{-9}	6.25×10^{-9}	3.45×10^{-9}	
1	GeV	2.35×10^{-9}	3.06×10^{-9}	2.63×10^{-9}	2.80×10^{-9}	2.75×10^{-9}	2.00×10^{-9}	3.06×10^{-9}	1.81×10^{-9}	
2	GeV	2.50×10^{-10}	3.03×10^{-10}	2.50×10^{-10}	3.75×10^{-10}	2.70×10^{-10}	1.65×10^{-10}	3.03×10^{-10}	2.37×10^{-10}	
4	GeV	2.50×10^{-11}	2.55×10^{-11}	1.93×10^{-11}	4.85×10^{-11}	2.23×10^{-11}	1.70×10^{-11}	2.55×10^{-11}	3.03×10^{-11}	

TABLE 1.5

DIFFERENTIAL PROBABILITIES FOR MUON INITIATED DPP PROCESS OF LEAD AT E = 100 GeV MUON ENERGY

(cm^2/gm MeV)

Transfered Energy	BF cross section	MUT cross section α =2, n = 4	MUT cross section α =1, n = 4	Kobayakawa cross section derived from MUT	Ternovskii cross section	Kel'ner cross section	Kel'ner Kotov cross section	Wright cross section derived from Kel'ner Kotov	Bhabha cross section
3.16 MeV	5.00×10^{-5}			2.97×10^{-4}		5.00×10^{-5}	5.20×10^{-5}	5.24×10^{-4}	9.01×10^{-6}
5 MeV	7.45×10^{-5}	1.01×10^{-4}	7.00×10^{-5}	1.85×10^{-4}	7.60×10^{-5}	7.45×10^{-5}	7.30×10^{-5}	3.35×10^{-4}	7.31×10^{-5}
10 MeV	6.95×10^{-5}	7.90×10^{-5}	5.88×10^{-5}	9.21×10^{-5}	6.50×10^{-5}	7.00×10^{-5}	6.55×10^{-5}	1.61×10^{-4}	7.45×10^{-5}
20 MeV	4.55×10^{-5}	5.25×10^{-5}	4.00×10^{-5}	4.48×10^{-5}	4.45×10^{-5}	4.78×10^{-5}	4.15×10^{-5}	7.75×10^{-5}	5.08×10^{-5}
40 MeV	2.50×10^{-5}	3.20×10^{-5}	2.46×10^{-5}	2.12×10^{-5}	2.60×10^{-5}	2.73×10^{-5}	2.30×10^{-5}	3.60×10^{-5}	2.80×10^{-5}
80 MeV	1.19×10^{-5}	1.56×10^{-5}	1.29×10^{-5}	9.56×10^{-6}	1.29×10^{-5}	1.38×10^{-5}	1.12×10^{-5}	1.56×10^{-5}	1.33×10^{-5}
100 MeV	8.96×10^{-6}	1.16×10^{-5}	9.50×10^{-6}	7.27×10^{-6}	9.50×10^{-6}	1.01×10^{-5}	8.50×10^{-6}	1.17×10^{-5}	1.02×10^{-5}
200 MeV	3.45×10^{-6}	4.17×10^{-6}	3.50×10^{-6}	2.88×10^{-6}	3.50×10^{-6}	3.90×10^{-6}	3.37×10^{-6}	4.32×10^{-6}	4.09×10^{-6}
400 MeV	1.20×10^{-6}	1.39×10^{-6}	1.59×10^{-6}	9.50×10^{-7}	1.59×10^{-6}	1.36×10^{-6}	1.10×10^{-6}	1.31×10^{-6}	1.34×10^{-6}
800 MeV	3.22×10^{-7}	3.57×10^{-7}	2.99×10^{-7}	2.60×10^{-7}	2.99×10^{-7}	3.48×10^{-7}	3.00×10^{-7}	3.18×10^{-7}	1.80×10^{-7}
1 GeV	2.01×10^{-7}	2.21×10^{-7}	1.86×10^{-7}	1.63×10^{-7}	1.86×10^{-7}	2.15×10^{-7}	1.91×10^{-7}	1.91×10^{-7}	
2 GeV	3.90×10^{-8}	4.29×10^{-8}	3.63×10^{-8}	3.23×10^{-8}	3.63×10^{-8}	4.17×10^{-8}	3.81×10^{-8}	3.46×10^{-8}	
4 GeV	6.60×10^{-9}	7.46×10^{-9}	6.41×10^{-9}	5.37×10^{-9}	6.40×10^{-9}	7.19×10^{-9}	6.50×10^{-9}	5.36×10^{-9}	
8 GeV	9.00×10^{-10}	1.08×10^{-9}	9.36×10^{-10}	7.83×10^{-10}	9.18×10^{-10}	1.02×10^{-9}	8.50×10^{-10}	7.55×10^{-10}	
10 GeV	4.57×10^{-10}	5.76×10^{-10}	5.07×10^{-10}	4.14×10^{-10}	4.84×10^{-10}	5.30×10^{-10}	4.41×10^{-10}	3.96×10^{-10}	
20 GeV	4.90×10^{-11}	6.52×10^{-11}	6.17×10^{-11}	5.53×10^{-11}	5.59×10^{-11}	5.42×10^{-11}	5.16×10^{-11}	5.19×10^{-11}	
40 GeV	5.10×10^{-12}	5.81×10^{-12}	5.62×10^{-12}	7.16×10^{-12}	6.17×10^{-12}	4.30×10^{-12}	5.20×10^{-12}	6.65×10^{-12}	

TABLE 1.6

DIFFERENTIAL PROBABILITIES FOR MUON INITIATED DPP PROCESS OF LEAD AT E = 1000 GeV MUON ENERGY

(cm^2/gm MeV)

Transfered Energy	KP cross section	MUT cross section $\alpha=2$, n = 4	MUT cross section $\alpha=1$, n =4	Kobayakawa cross section derived from MUT	Ternovskii cross section	Kel'ner cross section	Kel'ner Kotov cross section	Wright cross section derived from Kel' ner Kotov	Bhabha cross section
3.16 MeV	8.26×10^{-5}			3.45×10^{-4}		8.26×10^{-5}	8.30×10^{-5}	8.19×10^{-4}	1.31×10^{-5}
5 MeV	1.27×10^{-4}	1.46×10^{-4}	1.00×10^{-4}	2.18×10^{-4}	1.13×10^{-4}	1.27×10^{-4}	1.20×10^{-4}	5.25×10^{-4}	1.10×10^{-4}
10 MeV	1.11×10^{-4}	1.22×10^{-4}	8.48×10^{-5}	1.09×10^{-4}	1.01×10^{-4}	1.14×10^{-4}	1.11×10^{-4}	2.59×10^{-4}	1.20×10^{-4}
20 MeV	7.60×10^{-5}	9.00×10^{-5}	6.40×10^{-5}	5.42×10^{-5}	7.59×10^{-5}	8.28×10^{-5}	7.80×10^{-5}	1.29×10^{-4}	8.40×10^{-5}
40 MeV	4.50×10^{-5}	5.80×10^{-5}	4.32×10^{-5}	2.70×10^{-5}	4.73×10^{-5}	5.04×10^{-5}	4.44×10^{-5}	6.48×10^{-5}	5.08×10^{-5}
80 MeV	2.42×10^{-5}	3.19×10^{-5}	2.57×10^{-5}	1.33×10^{-5}	2.57×10^{-5}	2.83×10^{-5}	2.37×10^{-5}	3.23×10^{-5}	3.48×10^{-5}
100 MeV	1.94×10^{-5}	2.45×10^{-5}	2.08×10^{-5}	1.06×10^{-5}	2.08×10^{-5}	2.27×10^{-5}	1.92×10^{-5}	2.49×10^{-5}	2.21×10^{-5}
200 MeV	9.00×10^{-6}	1.12×10^{-5}	9.18×10^{-6}	5.16×10^{-6}	9.18×10^{-6}	1.01×10^{-5}	9.00×10^{-6}	1.20×10^{-5}	1.02×10^{-5}
400 MeV	4.00×10^{-6}	4.84×10^{-6}	3.88×10^{-6}	2.44×10^{-6}	3.88×10^{-6}	4.36×10^{-6}	4.00×10^{-6}	5.57×10^{-6}	5.00×10^{-6}
800 MeV	1.65×10^{-6}	1.86×10^{-6}	1.53×10^{-6}	1.10×10^{-6}	1.53×10^{-6}	1.72×10^{-6}	1.62×10^{-6}	2.42×10^{-6}	2.01×10^{-6}
1 GeV	1.24×10^{-6}	1.38×10^{-6}	1.14×10^{-6}	8.38×10^{-7}	1.14×10^{-6}	1.29×10^{-6}	1.22×10^{-6}	1.81×10^{-6}	1.48×10^{-6}
2 GeV	4.40×10^{-7}	4.71×10^{-7}	3.92×10^{-7}	3.32×10^{-7}	3.92×10^{-7}	4.44×10^{-7}	4.40×10^{-7}	6.68×10^{-7}	4.45×10^{-7}
4 GeV	1.40×10^{-7}	1.46×10^{-7}	1.22×10^{-7}	1.09×10^{-7}	1.21×10^{-7}	1.39×10^{-7}	1.45×10^{-7}	2.03×10^{-7}	8.00×10^{-8}
8 GeV	3.70×10^{-8}	3.77×10^{-8}	3.18×10^{-8}	2.99×10^{-8}	3.26×10^{-8}	3.59×10^{-8}	3.73×10^{-8}	4.90×10^{-8}	
10 GeV	2.34×10^{-8}	2.36×10^{-8}	1.99×10^{-8}	1.88×10^{-8}	1.92×10^{-8}	2.27×10^{-8}	2.30×10^{-8}	2.95×10^{-8}	
20 GeV	4.50×10^{-9}	4.50×10^{-9}	3.87×10^{-9}	3.72×10^{-9}	3.74×10^{-9}	4.37×10^{-9}	4.67×10^{-9}	5.35×10^{-9}	
40 GeV	7.40×10^{-10}	7.40×10^{-10}	6.44×10^{-10}	6.19×10^{-10}	6.36×10^{-10}	7.18×10^{-10}	7.30×10^{-10}	8.28×10^{-10}	
80 GeV	1.10×10^{-10}	1.12×10^{-10}	9.70×10^{-11}	9.02×10^{-11}	1.01×10^{-10}	1.10×10^{-10}	1.20×10^{-10}	1.17×10^{-10}	
100 GeV	5.89×10^{-11}	6.07×10^{-11}	5.30×10^{-11}	4.77×10^{-11}	5.65×10^{-11}	6.01×10^{-11}	6.10×10^{-11}	6.12×10^{-11}	
200 GeV	7.00×10^{-12}	7.70×10^{-12}	6.58×10^{-12}	6.37×10^{-12}	7.90×10^{-12}	7.70×10^{-12}	7.58×10^{-12}	8.02×10^{-12}	
400 GeV	7.30×10^{-13}	9.78×10^{-13}	8.50×10^{-13}	8.27×10^{-13}	9.81×10^{-13}	9.78×10^{-13}	8.03×10^{-13}	1.03×10^{-12}	

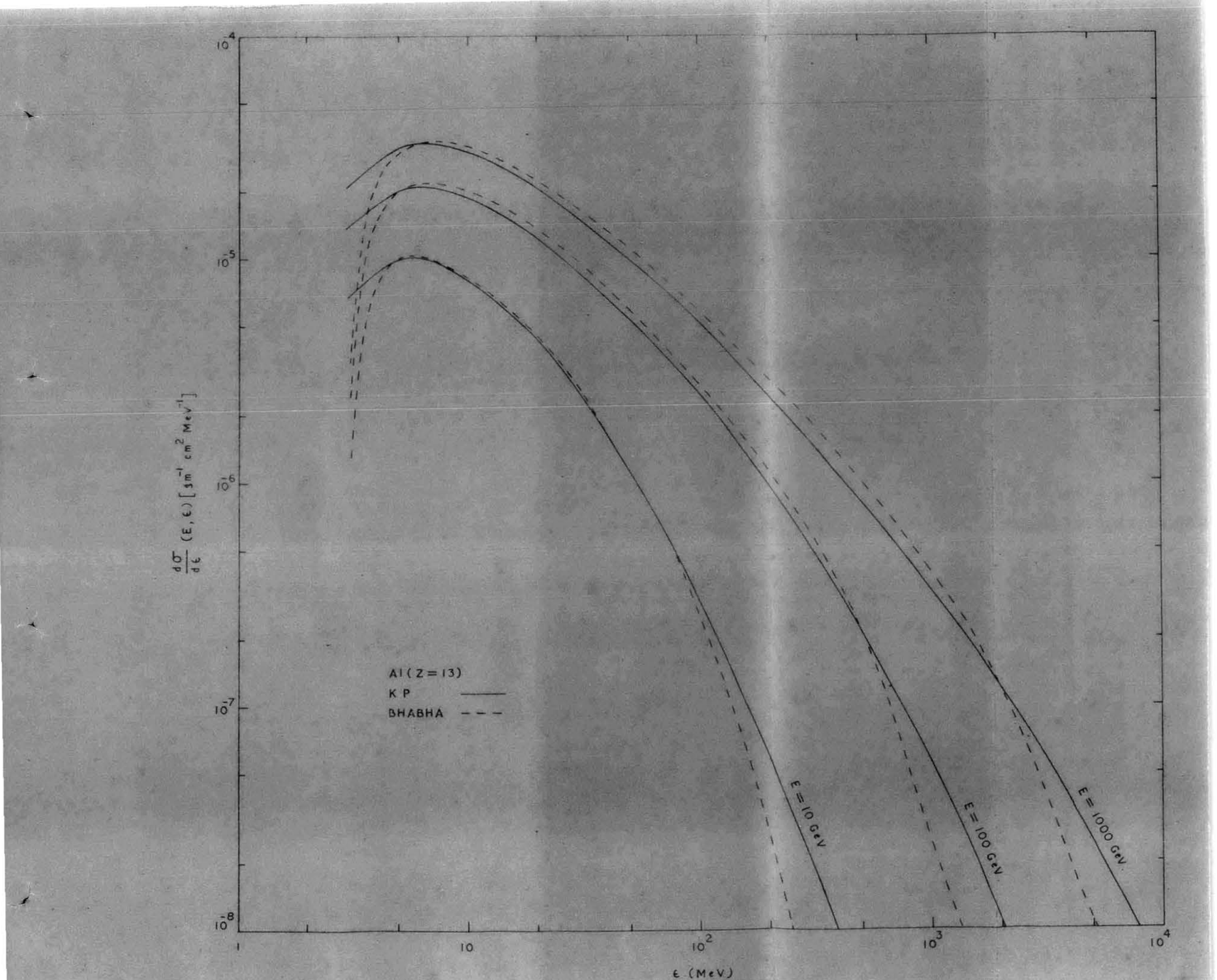
$\frac{d\sigma}{d\epsilon}(E,\epsilon)$ [gm^{-1} cm^2 MeV^{-1}]
10^{-4}
10^{-5}
10^{-6}
10^{-7}
10^{-8}
Al (Z = 13)
K P
BHABHA
E = 10 GeV
E = 100 GeV
E = 1000 GeV
1
10
10^2
10^3
10^4
ε (MeV)

FIG-1.2

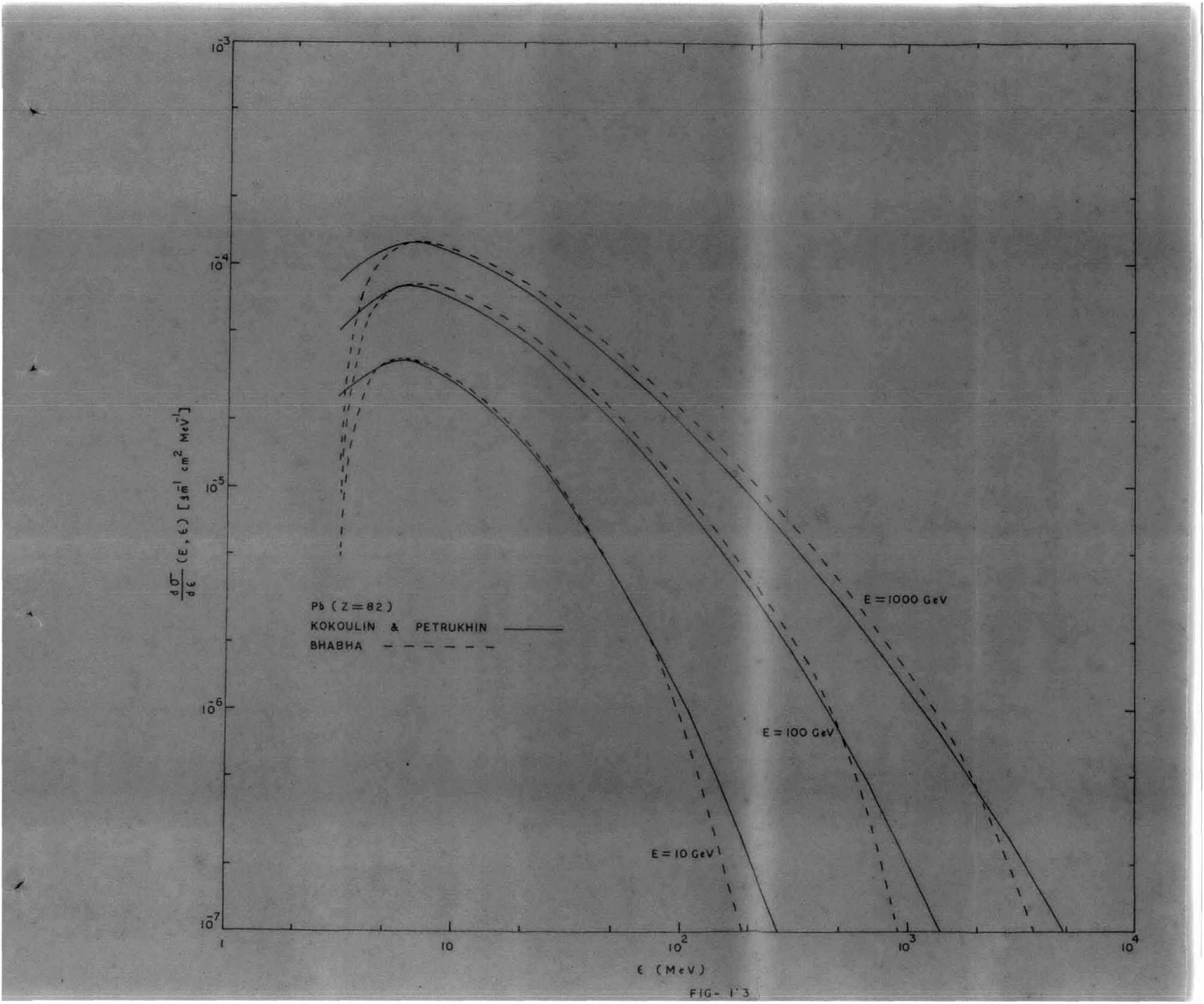
10^{-3}
10^{-4}
10^{-5}
10^{-6}
10^{-7}
$\frac{d\sigma}{d\epsilon}(E,\epsilon)$ [gm^{-1} cm^2 MeV^{-1}]
Pb (Z = 82)
KOKOULIN & PETRUKHIN
BHABHA
E = 1000 GeV
E = 100 GeV
E = 10 GeV
1
10
10^2
10^3
10^4
ϵ (MeV)

FIG- 1·3

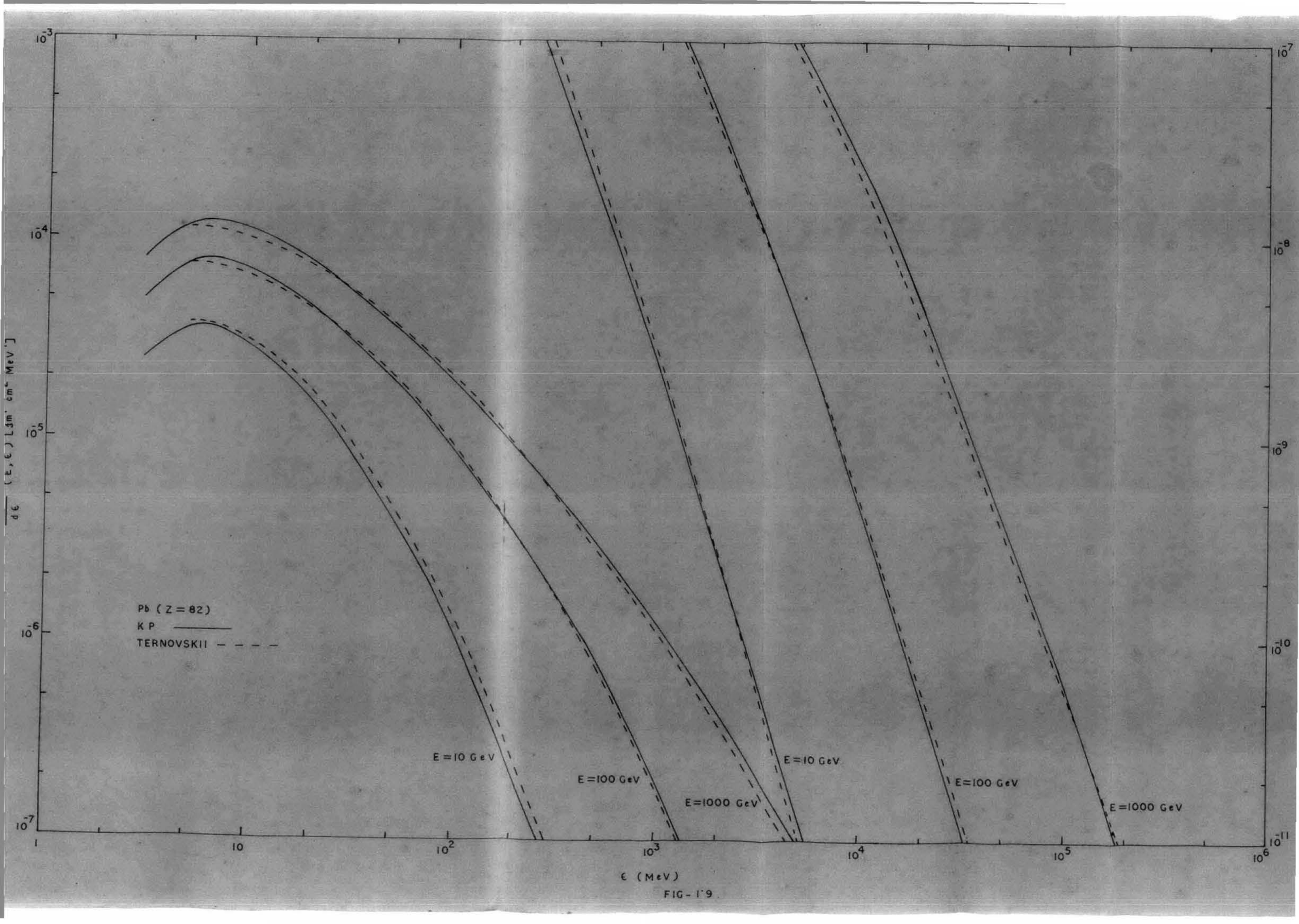
$\frac{d\epsilon}{dx}(E,\epsilon)$ [Lgm^{-1} cm^2 MeV^{-1}]
10^{-3}
10^{-4}
10^{-5}
10^{-6}
10^{-7}
10^{-7}
10^{-8}
10^{-9}
10^{-10}
10^{-11}
Pb (Z = 82)
K P
TERNOVSKII
E = 10 GeV
E = 100 GeV
E = 1000 GeV
E = 10 GeV
E = 100 GeV
E = 1000 GeV
1
10
10^2
10^3
10^4
10^5
10^6
ε (MeV)

FIG - 1·9

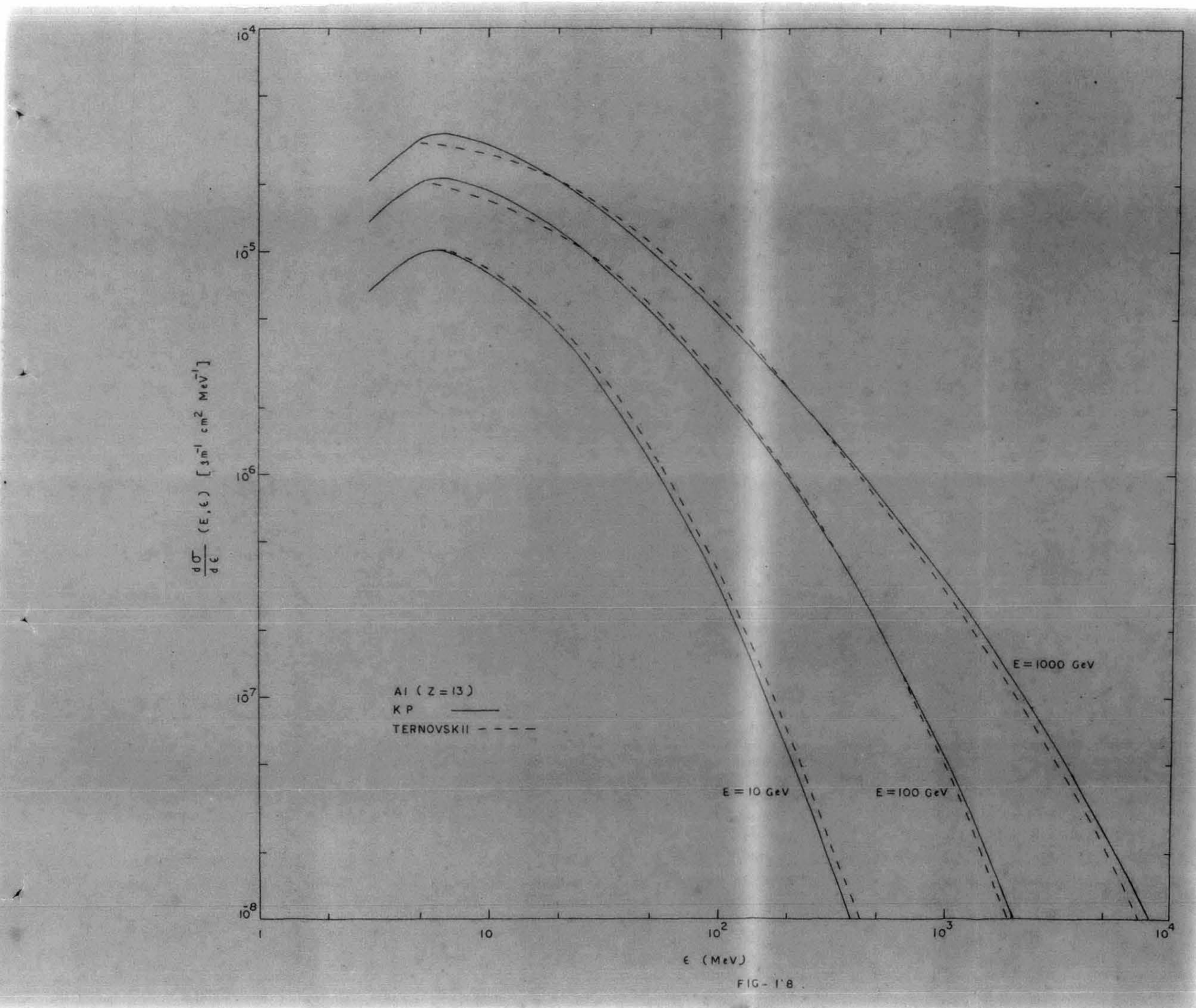
$\frac{d\sigma}{d\epsilon}$ (E,ε) [gm^{-1} cm^2 MeV^{-1}]
10^{-4}
10^{-5}
10^{-6}
10^{-7}
10^{-8}
Al (Z = 13)
K P
TERNOVSKII
E = 10 GeV
E = 100 GeV
E = 1000 GeV
1
10
10^2
10^3
10^4
ε (MeV)

FIG- 1'8 .

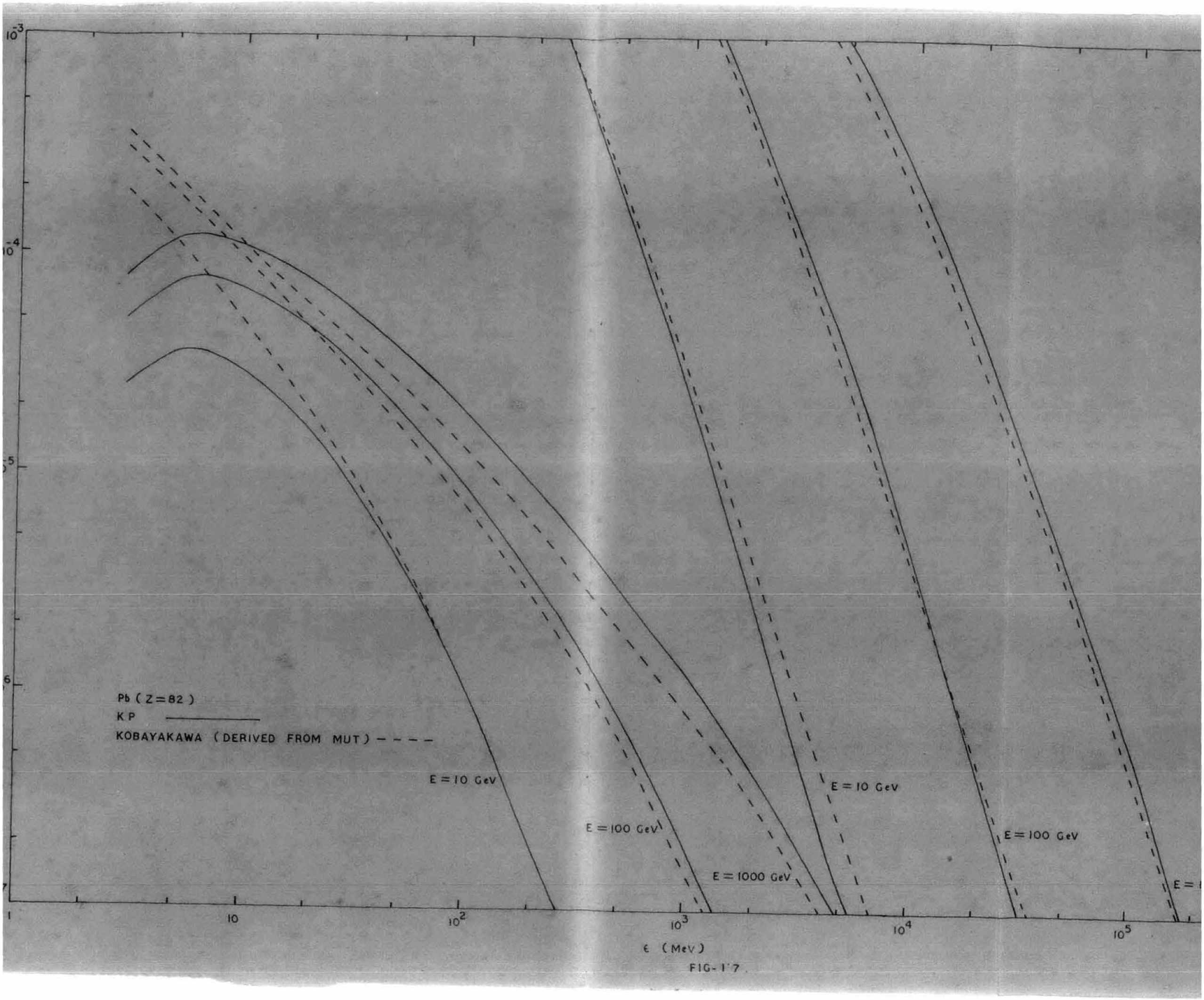
10^{-3}
10^{-4}
10^{-5}
10^{-6}
10^{-7}
Pb (Z=82)
K P
KOBAYAKAWA (DERIVED FROM MUT)
E = 10 GeV
E = 100 GeV
E = 1000 GeV
E = 10 GeV
E = 100 GeV
E =
1
10
10^2
10^3
10^4
10^5
ε (MeV)

FIG-17

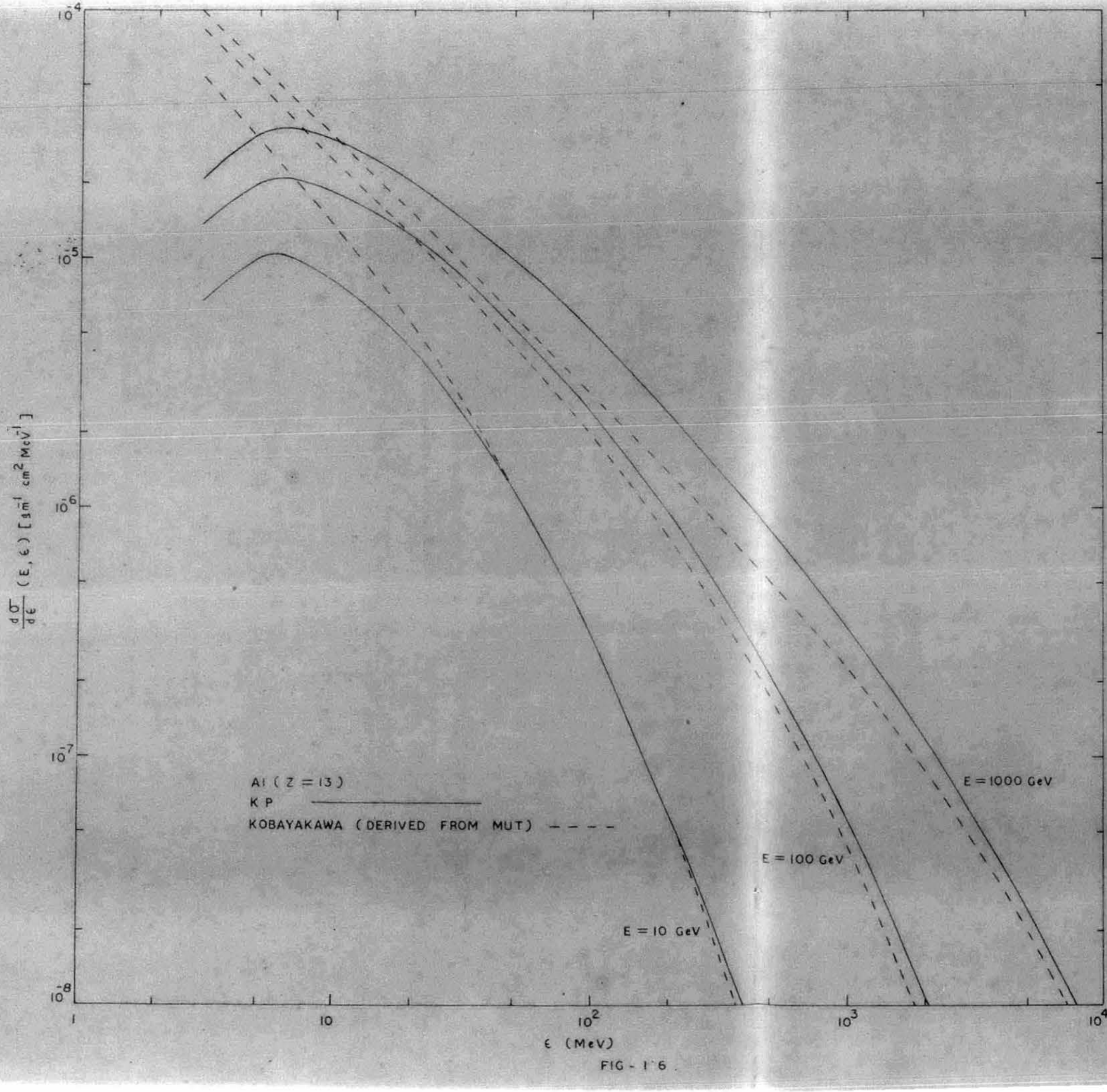
10^{-4}
10^{-5}
10^{-6}
10^{-7}
10^{-8}
$\frac{d\sigma}{d\epsilon}(E,\epsilon)$ [gm^{-1} cm^2 MeV^{-1}]
Al (Z = 13)
K P
KOBAYAKAWA (DERIVED FROM MUT)
E = 10 GeV
E = 100 GeV
E = 1000 GeV
1
10
10^2
10^3
10^4
ϵ (MeV)

FIG - 1 6

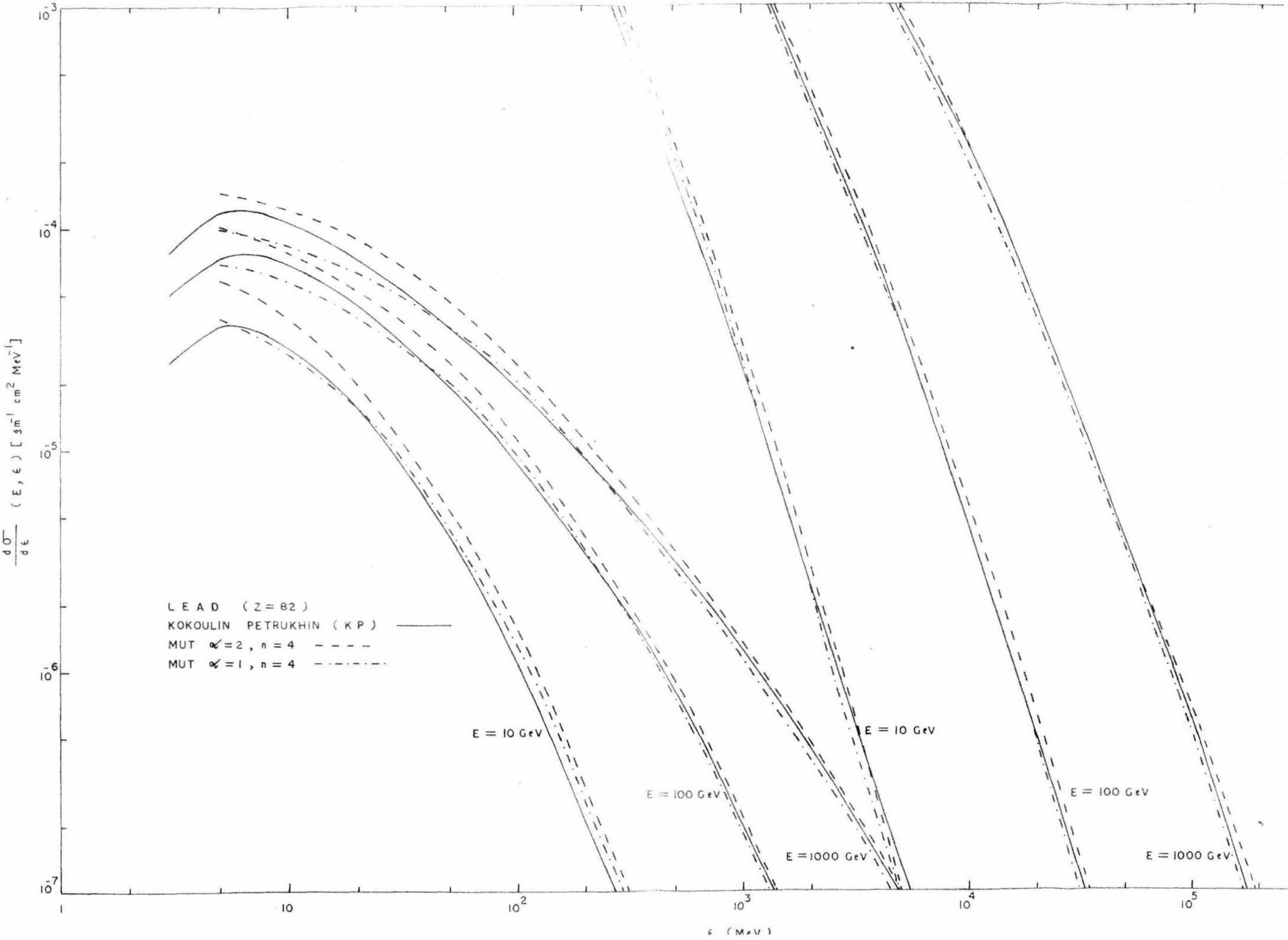
$\frac{d\sigma}{d\epsilon}$ (E, ε) [gm^{-1} cm^2 MeV^{-1}]
10^{-3}
10^{-4}
10^{-5}
10^{-6}
10^{-7}
1
10
10^2
10^3
10^4
10^5
ε (MeV)
LEAD (Z = 82)
KOKOULIN PETRUKHIN (KP) ——
MUT ∝ = 2 , n = 4 - - - -
MUT ∝ = 1 , n = 4 - · - · - ·
E = 10 GeV
E = 100 GeV
E = 1000 GeV
E = 10 GeV
E = 100 GeV
E = 1000 GeV

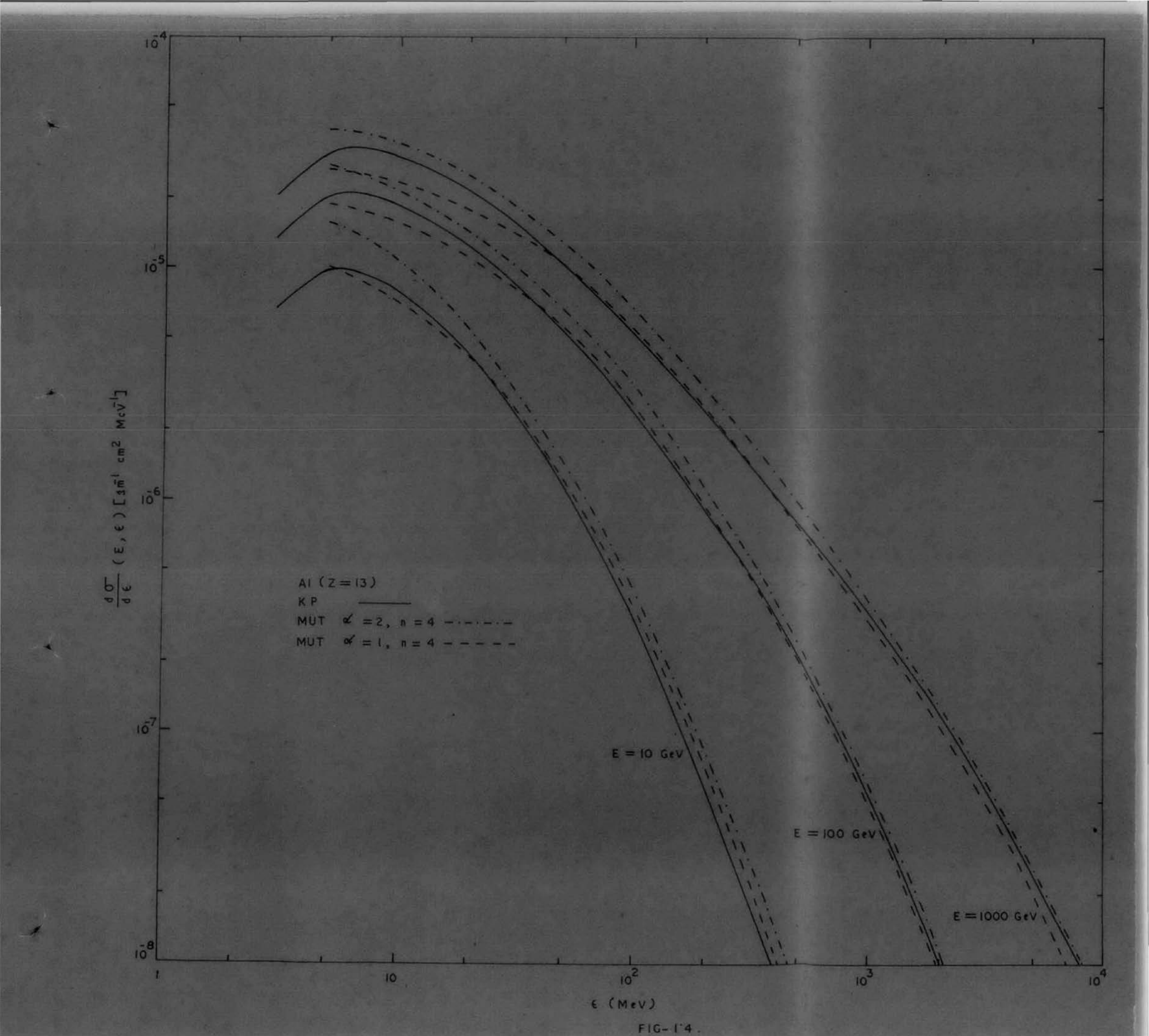
$\frac{d\sigma}{d\epsilon}(E,\epsilon)$ [gm^{-1} cm^2 MeV^{-1}]
10^{-4}
10^{-5}
10^{-6}
10^{-7}
10^{-8}
1
10
10^2
10^3
10^4
ϵ (MeV)
Al (Z=13)
KP
MUT α =2, n = 4
MUT α = 1, n = 4
E = 10 GeV
E = 100 GeV
E = 1000 GeV

FIG- 1·4 .

1.11.2 KP cross section with MUT cross section (figs. 1.4 and 1.5, tables 1.1 - 1.6)

Compared to MUT differential cross section (α =2) the KP cross section are lower and can possibly be distinguished in careful experiments at least below and energy transfer of 100 MeV in medium and high Z target elements. MUT cross section (α =1) are distinguishable from KP cross sections at low energy transfer for high muon energies from 100 GeV.

1.11.3 KP cross section with Kobayakawa cross section (figs.1.6 and 1.7, tables 1.1 - 1.6)

The MUT formula as modified by Kobayakawa was used in the analysis of some recent experiments. Compared to KP cross sections the modified MUT cross sections are much higher at very low energy transfer ($<$ 10MeV) for all primary energy. The situation is same at very higher energy transfer region except at the intermediate regions where the KP cross sections are higher. This trained of behavior is same for low and high Z target materials.

1.11.4 KP cross section with Fernovskii cross section (figs.1.8 and 1.9, tables 1.1 to 1.6)

Agreement between differential cross section according to KP and Fernovskii treatment is quite good over all energy regions considered in the present work. It may also be noted from table that MUT (α =1) cross section are in

Pb (Z = 82)
KP ——————
WRIGHT (DERIVED FROM KEL'NE KOTOV) - - - -

E = 10 GeV
E = 100 GeV
E = 1000 GeV

$d\epsilon$ [cm^{-1} MeV^{-1}]

ϵ (MeV)

FIG. 1.15

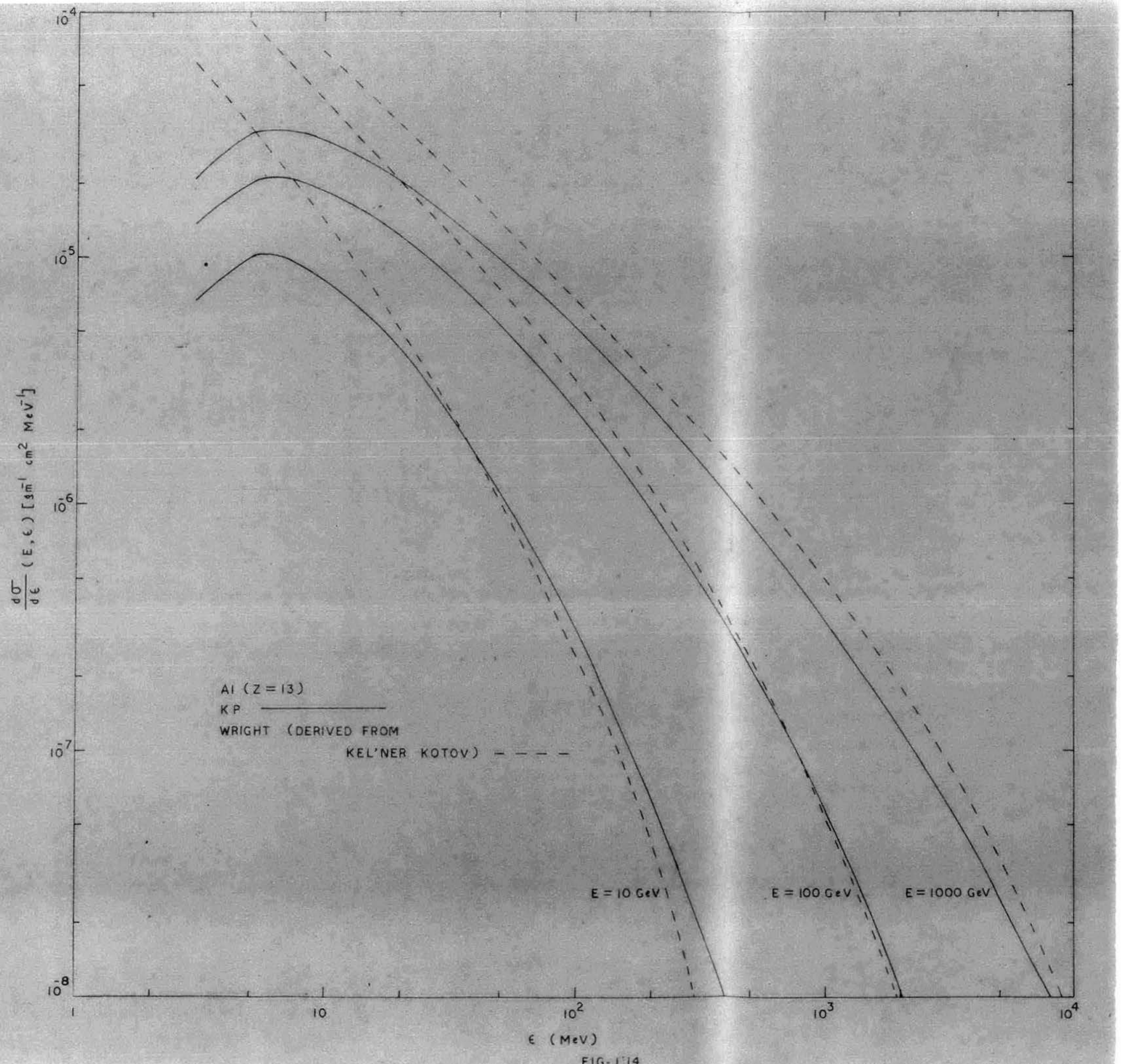
10^{-4}
10^{-5}
10^{-6}
10^{-7}
10^{-8}
$\frac{d\sigma}{d\epsilon}(E,\epsilon)$ [gm^{-1} cm^2 MeV^{-1}]
Al (Z = 13)
KP
WRIGHT (DERIVED FROM KEL'NER KOTOV) - - - -
E = 10 GeV
E = 100 GeV
E = 1000 GeV
1
10
10^2
10^3
10^4
ϵ (MeV)

FIG-1.14

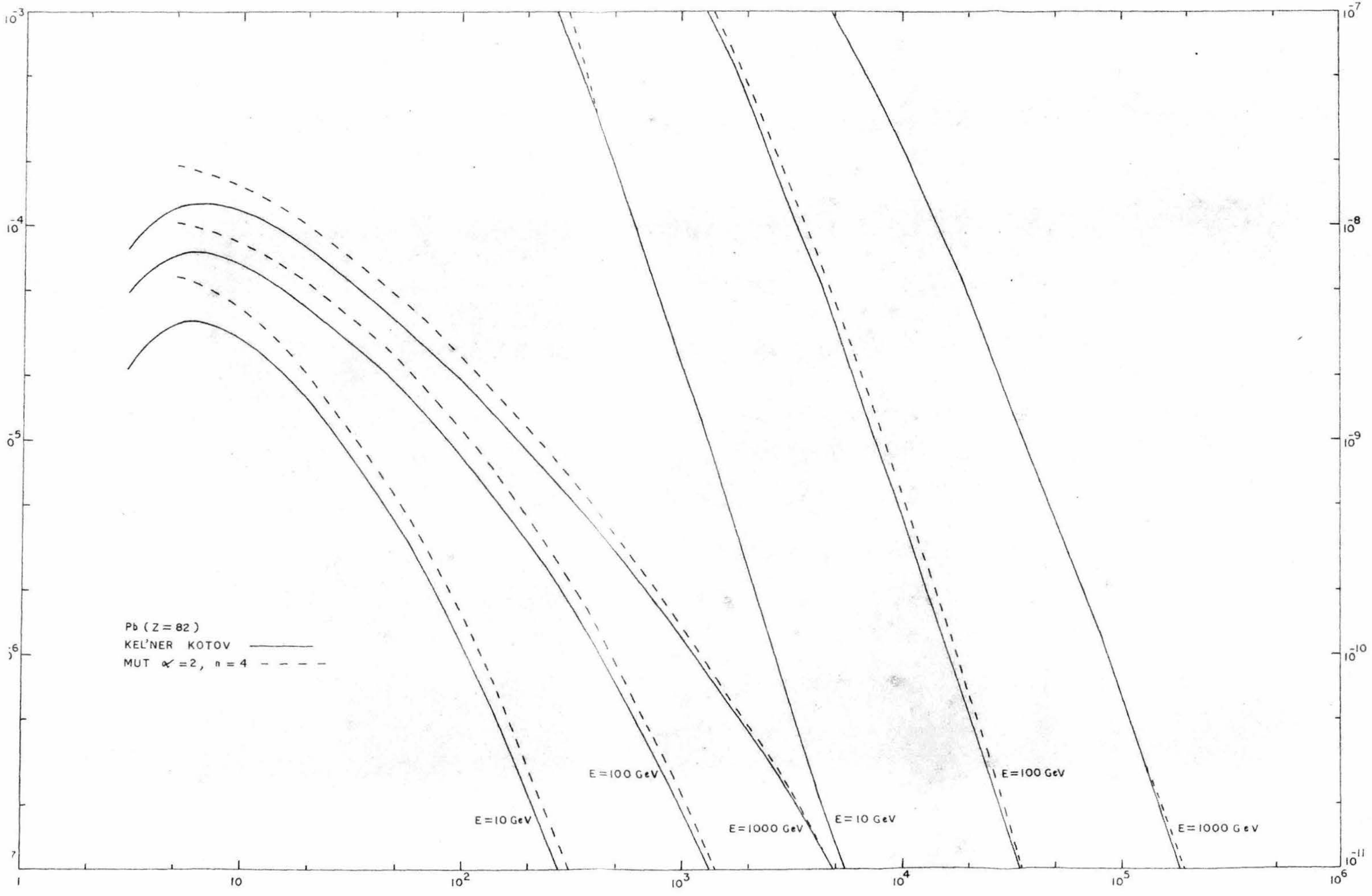
Pb (Z = 82)
KEL'NER KOTOV
MUT ∝ = 2, n = 4
E = 10 GeV
E = 100 GeV
E = 1000 GeV
E = 10 GeV
E = 100 GeV
E = 1000 GeV
ϵ (MeV)

FIG - 113

10^{-4}

10^{-5}

10^{-6}

10^{-7}

10^{-8}

$\frac{d\sigma}{d\epsilon}(E,\epsilon)$ [$3m^{-1}$ cm^2 MeV^{-1}]

Al(Z = 13)

KEL'NER KOTOV ——

MUT $\alpha = 2, n = 4$ - - - -

E = 10 GeV

E = 100 GeV

E = 1000 GeV

1

10

10^2

10^3

10^4

ϵ (MeV)

FIG 1.12

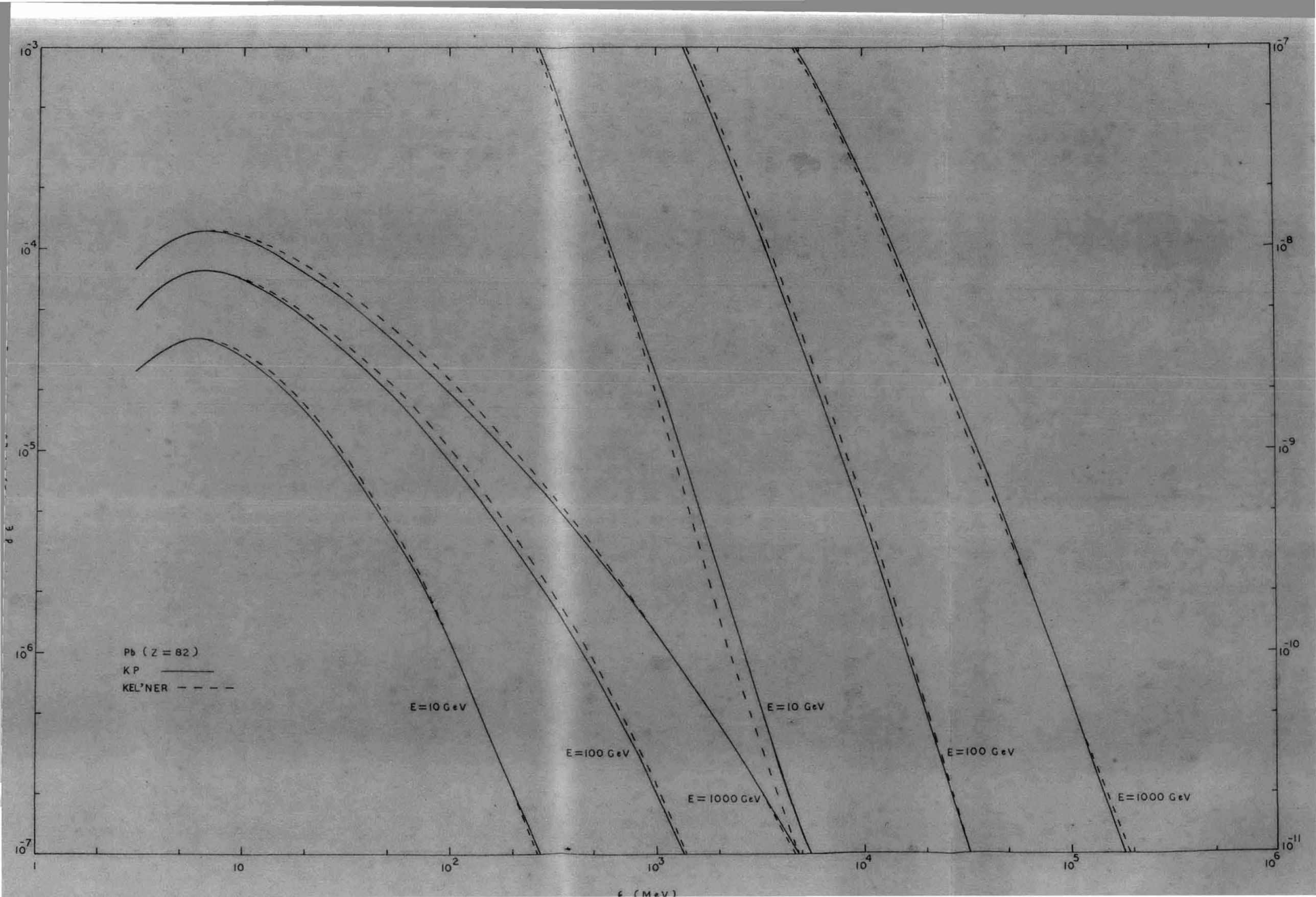
10^{-3}
10^{-4}
10^{-5}
10^{-6}
10^{-7}
10^{-7}
10^{-8}
10^{-9}
10^{-10}
10^{-11}
dε
Pb (Z = 82)
KP
KEL'NER - - - -
E=10 GeV
E=100 GeV
E=1000 GeV
E=10 GeV
E=100 GeV
E=1000 GeV
1
10
10^2
10^3
10^4
10^5
10^6
ε (MeV)

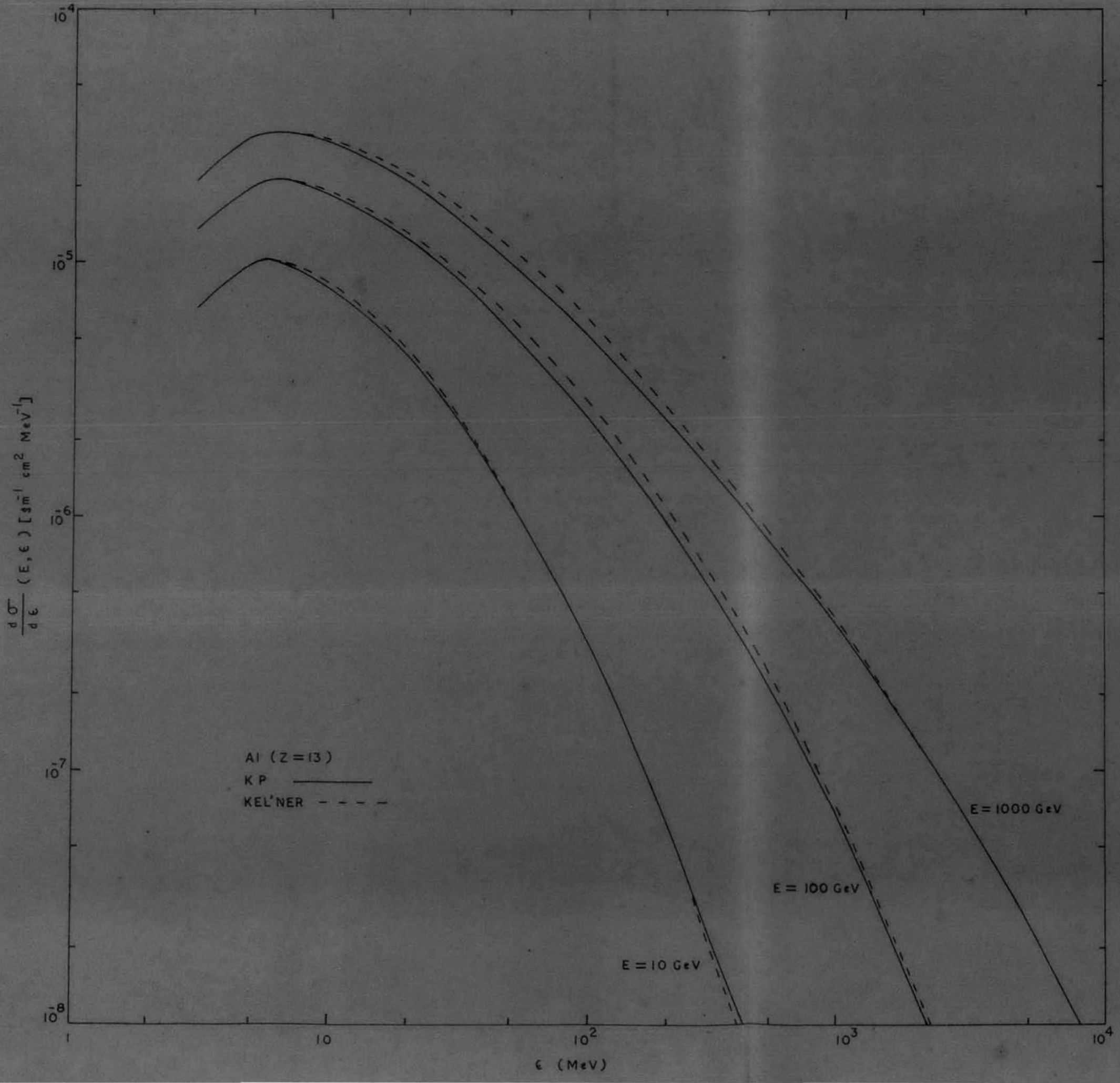
10^{-4}
10^{-5}
10^{-6}
10^{-7}
10^{-8}
$\frac{d\sigma}{d\epsilon}(E,\epsilon)$ [gm^{-1} cm^2 MeV^{-1}]
Al (Z = 13)
KP
KEL'NER
E = 10 GeV
E = 100 GeV
E = 1000 GeV
1
10
10^2
10^3
10^4
ϵ (MeV)

excellent agreement with Ternovskii cross section in the energy transfer range which widens with increasing primary energy, starting from energy transfer of about 80 MeV.

1.11.5 KP cross section with Kel'ner cross section (figs.1.10 and 1.11, tables 1.1 - 1.6)

The trend of behavior of Kel'ner cross section with respect to KP cross section is generally same as that observed in Ternovskii cross section relative to KP cross section. This behavior is in accordance with the similarity in basic approaches of the treatments.

1.11.6 Kel'ner Kotov cross section (figs.1.12 and 1.13, tables 1.1 - 1.6)

The Kel'ner Kotov cross section is practically indistinguishable from KJ cross section. In comparison with MUT (α=2) cross section Kel'ner Kotov cross section is systemetically lower, the difference decreasing with increasing energy transfer. This trend of behavior is same for low and high Z target atoms.

1.11.7 KP cross section with Wright cross section (derived from Kel'ner Kotov, figs.1.14 and 1.15, tables 1.1 - 1.6)

The formula (1.23) has been used recently in many analysis (ref. Kobayakawa 13th.Int.Conf. on Cosmic-rays, Denver, 1973).

We find that this formula predicts cross section much higher than KP cross section at lower energy transfer domain which widens gradually with increasing primary energy. The difference gradually decreases with increasing energy transfer. Compared to other cross section this cross section is also much higher at low energy transfer and there is significant deviation at other energy transfer except for some agreement in the case of MUT ($\alpha = 2$) cross section over a very small energy transfer range above 80 MeV.

1.12 Conclusion

After a critical re-evaluation of various theoretical treatments for the DPP process, we arrive at the following conclusions

1) Above an energy transfer of 5 MeV, Bhabha's theory of muons initiated DPP process predicts cross sections very close to those predicted by the exact KP theory over an energy transfer domain which expands gradually with increasing muon energy. Above this domain Bhabha's differential cross section distribution falls sharply below that of KP distribution. This trend of behavior is maintained in all targets ranging from carbon to lead and for all muon energies. The energy transfer domain of agreement is from 5 MeV to about 100 MeV at 10 GeV primary energy, extends to 500 MeV for 100 GeV primary

energy and to 2 GeV when the primary energy is 1000 GeV. Below 5 MeV energy transfer Bhabha's cross section decreases very sharply with the decrease in energy transfer.

2) MUT (α =2) cross section, which have been extensively used in the past experiments are somewhat higher than both KP and Bhabha's cross section in the intermediate energy transfer region starting from 5 MeV to a upper value which increases gradually with increasing primary energy. Above this upper value, difference is maintained which is very small and is almost constant. MUT (α =1) cross section, however, is closer to KP cross section at muon energies upto 100 GeV for all energy transfer. At higher muon energies, MUT (α =1) cross section upto energy transfer upto 20 MeV relative to KP cross section is lower than those below 100 GeV.

3) The trend of behavior of Ternovskii cross section is almost the same as that of MUT (α =1) cross section.

4) The interrelation between Kel'ner, Kel'ner Kotov and KP cross section is found to be very close throughout the energy transfer domain and primary energy range except for some minor differences.